EFFECT OF *Aspergillus niger* ON MECHANICAL, DIFFUSION AND THERMAL PROPERTIES OF HIGH DENSITY POLYETHYLENE/CELLULOSE BLEND

WASWA MICHAEL NAKITARE

[B.Ed (SC.) (Hons.)]

I56/CE/11194/2007

A thesis submitted in partial fulfillment of the requirements for the award of the Degree of Master of Science, in the School of Pure and Applied Sciences of Kenyatta University

August 2013

DECLARATION

I hereby declare that this thesis is the result of my own original research work and has not been presented for a degree in any other university or any other award

WASWA MICHAEL NAKITARE ……. …….....

Department of Physics, Sign Date

Kenyatta University,

P.O Box 43844 – 000100,

Nairobi, Kenya.

We confirm that the candidate, under our supervision, carried out the work reported in this thesis

DR. A.S MERENGA …… …….....

Department of Physics, Sign Date

Kenyatta University,

P.O Box 43844 – 000100,

Nairobi, Kenya.

DR. C.M MIGWI …….. …….....

Department of Physics, Sign Date

Kenyatta University,

P.O Box 43844 – 000100,

Nairobi, Kenya.

DEDICATION

This thesis is dedicated to my dear wife Christine and my beloved children Jeanette and Jael.

.

ACKNOWLEDGEMENTS

I would like to express my gratitude to all those who gave me the opportunity to complete this thesis. I am deeply indebted to Dr. A.S MERENGA and Dr. C.M MIGWI; department of physics, Kenyatta University, for their valuable guidance, support and encouragement which helped me throughout my research. They had been very kind and patient while suggesting the outlines of this project and correcting my doubts.

Many thanks to the technical staff of Plants and Microbial Science of Kenyatta University, especially Ms. Mercy Ndundu and Mr. Roy Mulanda who assisted me a great deal in isolating the strain of *Aspergillus niger*, auto-claving and the subsequent inoculation process of my samples. Their co-operation and support was key in the completion of my work. I am also thankful to all the staff members of the physics department and postgraduate colleagues' whose support and advice smoothed the progress of this endeavour.

My family was very integral during this period. It gives me immense pleasure to express my deep sense of gratitude to my dear wife Christine for her unwavering support and understanding. I can never forget the support my children Jeanette and Jael; thank you.

TABLE OF CONTENTS

LIST OF TABLES

LIST OF FIGURES

LIST OF APPENDICES

ABBREVIATIONS, SYMBOLS AND ACRONYMS

CELL	Cellulose
D	Diffusivity
DMA	Dynamic mechanical analysis
DSC	Differential scanning calorimetry
DTG	Derivative thermo-gravimetric
E	Tensile modulus
E’	Storage modulus
E’’	Loss modulus (MPa)
E_a	Activation energy
FTIR	Fourier Transform Infra-red Spectroscopy
HDPE	High density polyethylene
J	Creep compliance
K	Boltzman constant
LDPE	Low density polyethylene
n	Reaction order
P	Un-inoculated HDPE
PDA	Potato dextrose agar
PE	Polyethylene
PF	Inoculated HDPE
PP	Polypropylene
PVA	Poly (vinyl alcohol)

SEM	Scanning electron microscopy
T	Absolute temperature (K)
T_c	Decomposition temperature
T_g	Glass transition temperature
TGA	Thermo-gravimetric analysis
T_m	Melting temperature
T_o	Vogel temperature
VFT	Vogel-Fulcher-Tamman
WLF	William-Landel-Ferry
Z	Frequency factor
α	Degree of conversion
δ	Phase lag
ε	Strain
η	Complex shear viscosity
σ	Stress
τ	Relaxation time
ω	Frequency

ABSTRACT

Plastic materials, particularly polyethylene (PE) are the major source of environmental pollution. High density polyethylene (HDPE) is an essential industrial material in Kenya which is hard and non-biodegradable and hence persists in the environment for longer times. Wider application of HDPE in packaging and agriculture has raised serious issue of waste disposal and its pollution. In order to mitigate this, structural modification through blending with biopolymers is deemed to provide a solution. HDPE/starch blends have been found to posses undesirable properties; they have high diffusivity, less rigid and high thermal stability. Conversely, cellulose (CELL) is a linear polysaccharide with enhanced rigidity and higher thermal stability. This study focused on the effect of inoculating HDPE/CELL blends with *Aspergillus niger* on their mechanical, diffusion and thermal properties. HDPE granules and CELL powder from acacia cell-sap were used to prepare the samples by hot pressing their molten mixture. The samples were then exposed to a strain of *A. niger* for 60 days. Dynamic mechanical analysis (DMA) was carried out in single cantilever mode in frequency range from 1 to 30 H_Z and temperature range from -30 to 120 ^oC. Creep measurements were performed at 30 ^oC, 40 ^oC, 50 ^oC and 60 ^oC. A sample was displaced for 12 minutes and allowed to recover for another 12 minutes. Thermo-gravimetric analysis (TGA) measurements were done within a temperature range of 25 to 550 ^oC at a heating rate of 5^oC/minute. Diffusion measurements were done at 25 ^oC by dipping the samples in distilled water and mass increase monitored after every 7 days in a time span of 42 days. Viscoelastic behavior of HDPE/CELL blends showed two relaxation processes which were greatly affected by inoculation. The α process is assigned to glass transition while β process is assigned to inter-lamellar shear. The intensity of both α and β peaks significantly reduced on inoculation due to the degradation of the blends by *A.niger*. The β-relaxation was heavily affected by inoculation suggesting that microbial attack started in the crystalline-amorphous interface. Creep performance of the HDPE/CELL blends improved with CELL loading and decreased on inoculation due to destroyed matrix. William-Landel-Ferry (WLF) model offered a better long-term prediction based on the short-term creep data. Time-temperature superposition technique produced smooth master creep curves through horizontal shifts which was used to predict creep behavior of the samples extending to 10^5 s. Thermo-gravimetric thermo-grams provided information about the mass loss, thermal decomposition and thermal stability of the blends. The non isothermal kinetics of the decomposition processes were analyzed using the Broido integral method. Thermal stability of the blends decreased with cellulose intake and on inoculation. The activation energies related to the correspondent reactions were calculated. Fick's second law was used to ascertain the diffusivity of water in the blends which increased with CELL intake and on inoculation. Cellulose thus lowers the thermal stability, improves hydophilicity of HDPE and reinforces it structural rigidity. Inoculation of the blends enhances biodegradability, lowers thermal stability and rigidity. In order to curb environmental pollution caused by plastics especially those used in packaging, use of CELL as a bio-filler and inoculating with *A.niger* at the pre-disposal stages is thus encouraged.

CHAPTER ONE

INTRODUCTION

1.1 Background to the research project

Synthetic polymers have become technologically significant and packaging is one industry that has been revolutionalized by oil based polymers such as polyethylene (PE), polypropylene (PP), polystyrene (PS), poly (ethylene-terephthalate) (PET) and poly (vinyl chloride) (PVC). Plastics' versatility allows it to be used in everything from the simple part, for example plastic bags, bottles and dolls to high-tech parts; cars, computer casing, electronic devices casing and many more (Reyes *et al*., 2000). Worldwide production of plastics rose to 280 million tons in the year 2011. This represents around 4 % increase from the year 2010 when 270 million tons were produced and almost half of that is discarded within a short time, remaining in garbage deposits and landfills. From 2010 to 2016, global plastic consumption is expected to grow by an average of about 4 % each year (Plastic Europe, 2010). In Kenya, over 4000 packaging bags are produced and only 10 % is recycled (Oyugi, 2007). According to the Ministry of Environment, (2009) Nairobi city releases 490 tons of plastic waste daily to its environs which has been a health hazard to city dwellers.

Polyethylenes (PE), alongside polypropylene (PP) are saturated polymers with a general expression C_nH_{2n} and are the most widely used linear hydrocarbon polymers. They have a very low water vapor transmission rate and most importantly, they are totally non-biodegradable, and therefore lead to environmental pollution, which pose serious ecological problems (Australian Marine Conservation Society, 2011). Industrially

applicable PE was first synthesized in 1993 by Eric Fawcett and Reginald Gibson at ICI chemicals (Trossarelli *et al*., 2003). Polyethylene has a varying range of densities from 0.91 to 0.97g/cm^3. Low density PE has branching at random places leading to low packing of the polymer chains, whereas the high density PE is more linear with minimal branching leading to high packing density. High density PE widely uses is attributed to its availability in different forms. It is affordable and has outstanding features such as regular chain structure that explains its high degree of crystallinity, robust mechanical properties, process ability and chemical resistance. Polyethylene is a product of polymerization of ethylene monomers formed in the presence of an organo-metallic compound as a catalyst and pressure (15-30 atm). HDPE has a melting point in the range of 400-408 K (Fried, 1995). It's a modulus of 6.897×10^8 Pa with good tensile strength, hardness and low permeability to gases and vapors (James, 1986). The increasing problem posed by plastics waste management has stimulated interest in the development of strategies to find out a solution to this environmental problem. Among them, efforts have been made in recent past to develop degradable materials to replace conventional synthetic polymers (Griffin, 1994).

Due to the myriad applications of plastics, production of biodegradable plastics is considered as a possible way to solve the solid waste problem. Compounding synthetic polymers with natural polymers such as starch, cellulose, lignin, chitin, and chitosan is a significant way to accelerate polymer degradation (Baker and Liu, 1998). One of the most widely employed methods to modify the polymer resins is to blend them. Physical blending is one such technique that has been reported to greatly influence the mechanical

properties of polymers (Kalfoglu, 1982). Polyethylene blended with cellulose is found to be a potential candidate to replace non-degradable thermoplastics. Cellulose is a hydrophilic polymer, mainly due to the hydroxyls it contains. In contrast, PE is hydrophobic. Because of this totally different polar character of the polymers, they are immiscible. Biodegradable plastics are plastics that can undergo a degradation process. They are defined as plastics with similar properties to conventional plastic but which can be decomposed after disposal to the environment by activity of micro-organisms (Raghavan, 1995., Tharanathan, 2003). Biodegradable polymers, during their usage must have same mechanical properties like synthetic polymers. However, they finally degrade to low molecular weight compounds such as water and carbon (IV) oxide. Microbial biodegradable plastics could be degraded into simpler particles such as H_2O and CO_2 by micro-organisms' activities. Bacteria and fungi are attracted to polyethylene/starch based blend (Rutkowska *et al.*, 2002). Biodegradation occurs when micro-organisms such as bacteria and fungi degrade a polymer in an aerobic and anaerobic environment. Hence biodegradation can be stated as the conversion of polymer to carbon (IV) oxide, methane, microbial cellular components and miscellaneous by-products, by micro-organisms (Raghavan, 1995). Micro-organisms break down the polymer chains and consume the material through several methods. In this study, *Aspergillus niger* was used to degrade HDPE/CELL blends. The mechanism of biodegradation involves the following stages:

i) Attachment of micro-organism to the surface of the polymer.

ii) Growth of micro-organism utilizing the polymer as the carbon source.

iii) Primary degradation and ultimate degradation of the polymer.

Several analytical techniques have been used to monitor the extent and nature of biodegradation. Dynamical Mechanical Analysis (DMA) is an integral technique that helps in understanding the polymeric material behavior under loads, compare properties of similar materials and characterize them. The DMA is a method of monitoring property changes in materials as they are cycled through a range of temperatures. It measures changes in mechanical behavior such as modulus and damping as a function temperature, time, frequency, stress or a combination of these parameters. It therefore provides a tool for studying the mechanical properties of injection-molded materials (Sepe, 1992). Thermal analysis can provide useful information about the irreversible changes in properties of polymers caused by degradation in microbial consortiums. DMA and TGA methods were employed in this study since they provide both qualitative and quantitative information about the degradation process. This study focuses on the effects of *Aspergillus niger* on the relaxation process, creep, thermal degradation, and diffusion of HDPE/CELL fungus inoculated blends.

1.2 Statement of research problem

With the growing concern about environmental pollution, the accumulation of plastics waste needs immediate resolution. Plastics packaging has become a major contribution to accumulation of plastics waste in landfills. There is therefore need to explore and develop new materials that can undergo enzymatic scission in order to curb environmental pollution. Increasing public concern over dwindling landfill space and accumulation of surface litter has promoted the development of degradable plastics. Biodegradable plastics offer one solution to managing the plastic waste menace. In the last five years,

there has been an increased interest in the production and use of fully biodegradable polymers with the main aim being replacement of non-biodegradable plastics especially those used in packaging. However, although these polymers posses the required properties, they are not widely used due to their cost. Therefore, many research attempts have been focused on use of blends of PE and biopolymers such as starch, cellulose, which are fully biodegradable. In addition, these materials are also very cheap and are produced from renewable- natural sources. Addition of cellulose as a filler in PE blend increases the biodegradability of the samples making it suitable for packaging industry. High content of cellulose in the HDPE matrix inoculated by the strain of *Aspergillus niger* will enhance its biodegradability. Cellulose is susceptible to microbial attack and thus when the HDPE/CELL blend samples are inoculated by *Aspergillus niger*, the polymer blend will be attacked leaving it full of holes. This form enables easier disintegration of the material into small pieces. It also increases the total surface area accessible to oxygen. As a result, oxidation of PE becomes easier. In this research work, the focus is on inoculating HDPE/CELL blend with *Aspergillus niger* and investigate their mechanical, diffusion and thermal properties. The hydroxyl groups in cellulose gave more insight into inter-chain interactions in the blends.

1.3 Objectives

1.3.1 Main objective

To establish the impact of *Aspergillus niger* on the dynamic mechanical analysis and diffusion properties of hot pressed samples of HDPE and cellulose samples.

1.3.2 Specific objectives

To determine the effect of inoculating HDPE/CELL blends by *A.niger* on:

a) Water uptake behavior of the HDPE/cellulose blends.

b) Activation energy and decomposition temperature of the HDPE/cellulose blends.

c) Creep compliance and creep strain of the HDPE/cellulose blends.

d) Loss and storage moduli of the HDPE/cellulose blends.

1.4 Rationale of the study

Non-degradable plastics accumulate in the environment at a rate of 80 million tones per year (Plastic Europe, 2010). Extensive use of non-biodegradable thermoplastics and the rate, at which they accumulate in the environment, makes mankind to realize the necessity to find its environmental impact. The rationale behind this research work was the predominant Acacia trees whose cell sap is rich in cellulose that could be blended with HDPE. Coupled with cellulose, is the availability of *Aspergillus niger* which fundamentally degrades several polymeric materials. Cellulose injects hydroliphic characteristics in the HDPE matrix hence enhancing the chances of biodegradation. Biodegradable plastics/polymers for example HDPE is seen by many as a promising solution to this problem because they are eco- friendly.

CHAPTER TWO

LITERATURE REVIEW

2.1 Microbial degradation

Microbial degradation results from the action of naturally occurring micro-organisms such as bacteria, fungi, algae etc. The product so formed is not visible and need not be screened after decomposing (Upreti *et al*., 2003). The production of biodegradable plastics that can get decomposed completely in nature has received remarkable attention globally as they are fully eco-friendly and helpful in waste landfill management. Additional of natural polymers to thermal plastics having long-term potential is one of the approaches to enhance biodegradability.

Shah *et al*. (1995) found that, various fungi and bacteria through starch hydrolysis, have consumed the starch granules present on the surface of the polymer. Holes and cracks were also observed on the surface of the hydrolyzed polymer in the SEM micrographs. Akaranta and Oku (1999) also confirmed that, the incorporation of starch in LDPE/starch blends promotes the growth of microbes on the surface of the films. The growth of the colony also increased with increase in the starch content of the films. According to Zuchoswka *et al*. (1999), fungi species *Penicillin funiculosum, Fusalium redolens and Aspergillus vesicolour* and soil microorganisms (mixed culture as well as *Rhodococcus rhodochrous, Cladosporium cladosporoides)* are reported to degrade polyethylene.

2.2 Studies involving Aspergillus species

Morancho *et al*. (2006) reported that *Aspergillus niger* was able to degrade commercially available PE. Differrential scanning calorimetry analysis showed reduction in the amorphous region of the polymer. According to Konduri *et al*. (2004) abiotically treated HDPE samples exposed to sample strains showed a greater reduction in tensile strength, breaking load and percentage of elongation compared to untreated HDPE. Ultra-Violet irradiated HDPE exposed to *Aspergillus oryzae, Aspergillus niger* and *Aspergillus flavus* showed 63 %, 46 % and 32 % reduction in tensile strength respectively. Percentage reduction elongation of 72 %, 52 % and 40 % respectively was also observed with treated HDPE.

Labuzek *et al*. (2003) investigated the biodegradation of LDPE film modified with Bionolle by fungi and noted that the modified PE film incubated with *Aspergillus niger* revealed regular yellow and brown spots on the surface of samples. The absence of small fragments of the film was observed after 20 days of cultivation and the samples grew thinner after 70 days. Equally, the percentage of weight loss increased significantly after 60 days. After the first 10 days the samples incubated with *Penicillium funiculosum* had whitened parts which indicated biodegradation over about 80 % of the sample area. LDPE film inoculated with *Penicillium funiculosum* exhibited little steady weight loss over the cultivation period. According to Kathiresan (2003), the microbial species found associated with the degrading of plastics and polyethylene bags were identified as bacteria, and eight fungal species of *Aspergillus*. The species that were predominant were *Streptococcus*, *Staphylococcus*, *Micrococcus* (Gram +ve), *Moraxella*, and *Pseudomonas*

(Gram –ve) and two species of fungi (*Aspergillus glaucus* and *A. niger*). Efficacy of the microbial species in degradation of plastics and polyethylene was analyzed in shaker cultures. Among the bacteria, *Pseudomonas* species degraded 20.54 % of polythene and 8.16 % of plastics in one-month period. Among the fungal species, *Aspergillus glaucus* degraded 28.80 % of polythene and 7.26 % of plastics in one-month period. Hence microbes are capable of degrading polythene and plastics.

2.3 Other studies involving microbial degradation

Some strains of the bacteria such as *Pseudomonas aeruginosa, Pseudomonas fluorescens* and fungi *Penicillium simplicissimum* have been reported as the most commonly used organisms for the plastic degradation (Tadros *et al.,* 1999 and Norman *et al.,* 2002). Sielick *et al*. (1978) studied the microbial degradation of [β- carbon-14] and 1, 3-diphenylbutane in soil and liquid enrichment cultures which was determined by evolution of carbon (IV) oxide. Metabolism of 1, 3-diphenylbutane appeared to involve the attack by a mono-oxygenease to form 2-phenyl-4-hydroxyphenylbutane. Mehdi *et al.* (2010) exposed starch based potato starch based LDPE to microorganisms and observed the weight changes for 8 months. In addition, FTIR and SEM were performed on the samples to validate the results. Fourier transform spectroscopy (FTIR) approved the result. Scanning electron microscope (SEM) and weight change after 84 days' exposure to *Pseudomonas aeruginosa* confirmed degradation by microorganisms. In addition, potato starch based LDPE was exposed to 8 different kinds of fungi and the degradation was studied visually. Result confirmed the microbial biodegradability of potato starch based LDPE blend in natural and laboratory condition.

Chiellin *et al*. (1999) investigated the biodegradability effects of micro-organic treatment on modified starch-based films. *B.subtillis, A.niger, A.oryzae, P. aeruginosa* and soil suspension were used because *Brevibacillus subtillis A.niger* and *A.oryzae* are amylase producing microorganisms and *P. aeruginosa* had a good degradability on PVA/starch films. During the exposure of the samples to the micro-organisms, microscopic colonies of the micro-organisms were observed on the surface of starch film and PVA /starch film, even within the first seven days of incubation.

Sahebnaza *et al*. (2006) studied biodegradation of LDPE by isolated landfill-source fungi in controlled solid waste medium. The fungi, including *Aspergillus fumigatus, Aspergillus terreus* and *Fusarium solani*, were isolated from samples taken from an aerobic aged municipal landfill in Tehran. Biodegradation was monitored using FT-IR and SEM. These fungi could degrade LDPE via the formation of a biofilm in a submerged medium. The results of FT-IR and SEM analyses show that *A. terreus* and *A. fumigatus*, despite the availability of other organic carbon of materials, could utilize LDPE as carbon source. Hadad *et al*. (2005) isolated thermophilic bacterium strain of *Brevibacillus borstelensis* for the degradation of LDPE and studied the effect of UV photo-oxidation on the extent of biodegradation of PE. Gilmore *et al*. (1993) carried degradation study of six different plastics and plastic blends in municipal wastewater. Samples consisted of 6 % starch in PP, 12 % starch in linear LDPE, 30 % polycaprolactone in LDPE, and poly(-hydroxybutyrate-co-hydroxyvalerate) (PHB/V). Microbially produced polyester in activated sludge of 5 months showed no signs of

degradation on blended samples except PHB/V, which showed a considerable loss of mass and a significant loss of tensile strength in municipal wastewater. Yamada *et al*. (2001) in their work reported the biodegradation of higher molecular weight untreated HDPE with molecular weight of up to 28,000 by *Penicillium simplicissimum*. Albertsson *et al*. (1998) reported that abiotically aged pure LDPE, LDPE/starch and LDPE-additives promoting degradation were characterized by the presence of several degradation products such as mono- and di-carboxylic acids and ketoacids. The products almost completely disappeared in the presence of *Arthobactor paraffineus* as a consequence of the assimilation of the degradation products by the bacteria strain.

Behjat *et al.,* (2009) in their studies made several blends of cellulose derived from bast part of kenaf (*Hibiscus cannabinus L.*) plant, with different thermoplastics, LDPE and HDPE, using a melt blending machine. Biodegradability of these blends was measured using soil burial test in order to study the rates of biodegradation of these polymer blends. It was found that the CELL/LDPE and CELL/HDPE blends were biodegradable in a considerable rate. The bio-composites with high content of cellulose had higher degradation rate. Although there has been considerable study of degradation of microbial consortiums in this area, there is no work that has been reported that study the dynamic mechanical analysis of hot pressed HDPE/CELL blends inoculated by *Aspergillus niger*. This work intends to give an insight of the mechanical, thermal and sorption properties of inoculated HDPE-CELL blends.

CHAPTER THREE

THEORETICAL BACKGROUND OF MEASURING TECHNIQUES

3.1 Dynamic mechanical analysis

Most polymers are viscoelastic in nature. Their mechanical properties exhibit a pronounced dependence on temperature and rate of deformation. There are so many products (for e.g; automobile tyre, vibration dampers etc that undergo cyclic stressing over a wide range of temperatures during their service life. DMA is a technique where small deformation is applied to a sample in a cyclic manner. The storage modulus, E', is the measure of the sample's elastic behavior and the loss modulus, E", is a measure of dissipation. The ratio of the loss to the storage moduli is the tan delta (phase angle) and is often called damping. It measures how well a material can get rid of energy and also how good a material will be at absorbing energy. It varies with the state of the material, its temperature, and with the frequency. According to (Strobl, 1997), the parameters used to specify mechanical properties of an isotropic medium in the absence of relaxation effects are stress (σ) and strain (ε) related as follows;

$$\sigma = E\varepsilon \tag{3.1}$$

where, E is the tensile modulus.

In the study of viscoelasticity, an oscillatory force (stress) is applied to the polymer and the resulting displacement (strain) is measured. In purely elastic materials the stress and strain occur in phase, so that the response of one occurs simultaneously with the other. In purely viscous materials, there is a phase difference between stress and strain, where strain lags stress by a 90 degree (π / 2 radian) phase lag. When a constant strain is applied

instantaneously to a sample and the stress induced measured as a function of time, the results are as shown in figure 3.0 (a) and (b).

a) Strain (ε) b) Stress (σ)

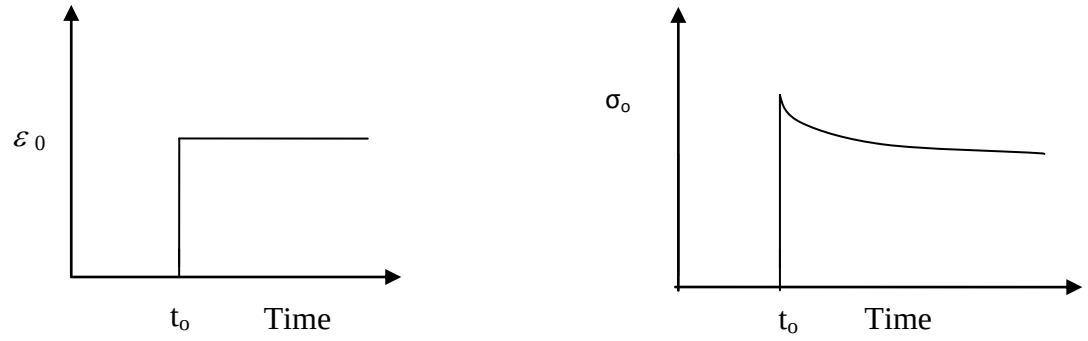

a) Applied strain b) Induced stress

Figure 3.0: a) Strain versus time (b) stress versus time.

The tensile stress has a maximum directly after the deformation and is proportional to the applied strain but decreases with time at a rate characterized by relaxation time (τ).

3.1.1 Dynamic mechanical measurement (complex modulus)

An alternative experimental procedure to creep and stress relaxation is to subject the specimen to an alternating strain and simultaneously measure the stress. For linear viscoelastic behavior, when the equilibrium is reached, the stress and strain varies sinusoidal, but the strain lags behind the stress. If stress $\sigma(t)$ is applied, then altered with time t and angular frequency ω then,

$$\sigma(t) = \sigma_o \sin \omega t \qquad (3.2)$$

where, σ_o is the amplitude.

For an ideal elastic body deformation instantly follows an applied stress, and consequently;

$$\varepsilon(t) = \varepsilon_o \sin \omega t \qquad (3.3)$$

Polymers are not ideal energy elastic bodies; they are viscoelastic materials. In such cases the deformation (strain) lags behind the applied stress as shown in figure 3.1.

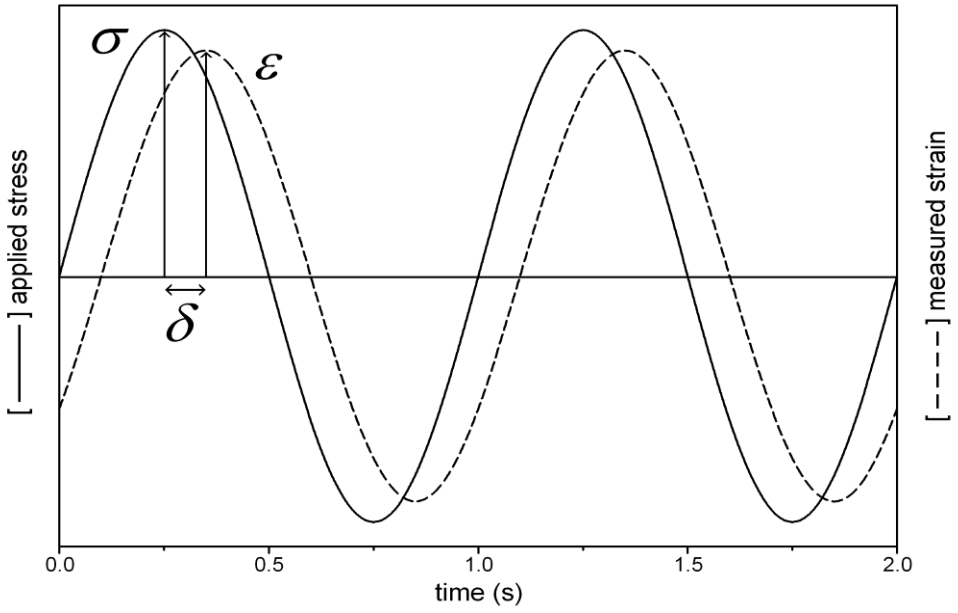

Figure 3.1: Stress and strain as a function of time with dynamic (sinusoidal) loading (Strain)

With ideal viscoelastic bodies, the resulting phase angle δ in the corresponding vector diagram can be assumed to be constant, such that the deformation or the strain is;

$$\varepsilon(t) = \varepsilon_o \sin \omega t \qquad (3.4)$$

$$\sigma(t) = \sigma_o \sin(\omega t + \delta) \qquad (3.5)$$

The stress vector can be considered to be the sum of two components. One component, $\sigma' = \sigma_o \cos \delta$, is in phase with the deformation, the other component, on the other hand, $\sigma'' = \sigma_o \sin \delta$, is out of phase. A modulus can be assigned to each of the components. The real modulus, or storage modulus, E', measures the rigidity and resistance to deformation of the sample. It is related to the complex modulus of rigidity E* by;

$$E' = \sigma' / \varepsilon_o = (\sigma_o / \varepsilon_o) \cos \delta = E^* \cos \delta \tag{3.6}$$

The imaginary, or loss modulus, E'', on the other hand, reflects the loss of useful mechanical energy through dissipation as heat. Similarly, E'' is given by;

$$E'' = \sigma'' / \varepsilon_o = E^* \sin \delta \tag{3.7}$$

The loss factor spectra can be quantitatively described by a superposition of model function,

$$E''(T) = \sum_{i=1}^{2} A_i \exp\left\{ -\frac{E_i}{kT} - \frac{T^2}{T_{m_i}^2} \exp\left[\frac{E_i}{k}\left(\frac{1}{T_{m_i}} - \frac{1}{T} \right) \right] \right\} \tag{3.8}$$

In this model function, A is a constant, k Boltzmann constant, T absolute temperature, T_m melting temperature, E is the activation energy and i refers to different processes which contribute to the mechanical response.

Introducing the complex variables, one may rewrite equations (3.4) and (3.5) as follows:

$$\varepsilon^* = \varepsilon_o \exp(j\omega t) \tag{3.9a}$$

$$\sigma^* = \sigma_o \exp\, j(\omega t + \delta) \tag{3.9b}$$

The complex modulus E* may be then expressed as;

$$E^*(\omega) = E'(\omega) + jE''(\omega) \tag{3.10}$$

where: $j^2 = -1$

Instead of following the deformation produced by a given stress, the sample can be strained and the resulting stress can be measured. The complex compliance J* = 1/E* is obtained in this case, and the storage and loss compliance are correspondingly given by

$$E' = J' / [(J')^2 + (J'')^2] \tag{3.11}$$

$$E'' = J'' / [(J')^2 + (J'')^2] \tag{3.12}$$

The complex dynamic shear modulus at frequency ω, E*(ω) expressed in Pa, is given by the ratio between the magnitude of the dynamic shear stress, τ(ω), and the magnitude of the applied dynamic shear strain, ε(ω).

$$E^*(\omega) = \tau(\omega)/\varepsilon(\omega) \tag{3.13}$$

The loss factor, storage modulus and loss modulus vary with frequency of loading as shown in figure 3.2.

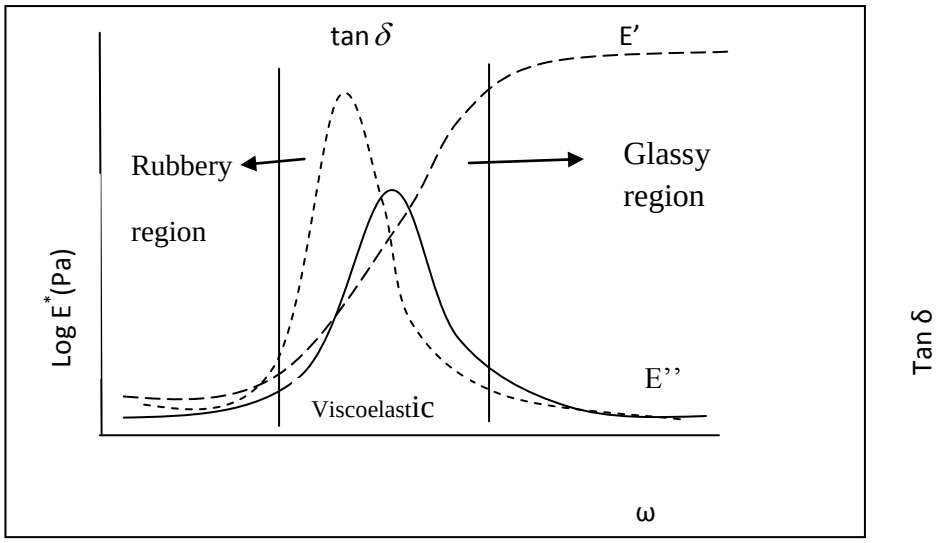

Figure 3.2: The complex modulus, E*=E'+jE", as a function of frequency.

At low frequency the polymer is rubber like and has a low storage modulus, which is independent of frequency. At high frequency, the polymer is glassy and the storage modulus is again independent of frequency. In the intermediate region where the material behaves viscoelastically, the storage modulus increases with increasing frequency. As the frequency is increased it becomes more difficulty for the chains to respond to the applied forces and tend to remain in a frozen state. A frozen system stores more energy than a free system (Ward and Hadley, 1993). The loss modulus is zero both at low and at high frequencies where stress and strain are in phase for the rubbery and glassy phases. In the intermediate viscoelastic region, the loss modulus increases to a maximum value then decreases. If the mechanical force applied has a low frequency compared to the transition rates in the system, establishment of a thermal equilibrium is rapid and the system can always remain in equilibrium, hence we encounter quasistatic conditions and observe the full relaxation strength. On the other hand when the frequency of the applied force is large compared to the transition rates, equilibrium cannot be established and the system

reacts to the average strain only, which is zero. Crossover from one regime to the other occurs at $\omega\tau \cong 1$(Hadley and Ward, 1993; Strobl, 1997). The phase angle, expressed as its *sine* or *tangent,* is an important parameter for describing the viscoelastic properties of a material. The complex, storage and loss moduli, and the phase angle are illustrated by the trigonometry of a right triangle, as shown in figure 3.3.

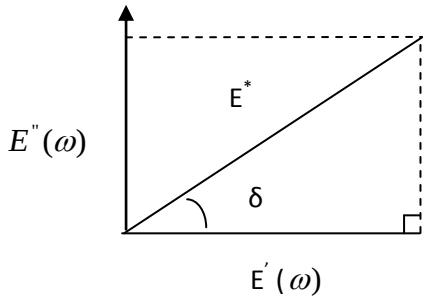

Figure 3.3: Relationship among dynamic moduli and phase angle.

It follows that the loss tangent can be calculated simply as the tangent of the phase angle, or alternatively, as the ratio of the loss to storage moduli:

$$\tan \delta = E'' / E' = \frac{1}{\omega\tau} \tag{3.14}$$

and that;

$$E^* = [(E')^2 + (E'')^2]1/2 \tag{3.15}$$

where *E**, is the ratio of the peak stress to the peak strain, reflects the total stiffness. The in-phase component of *E**, i.e. the shear storage modulus, E', represents the part of the input energy which is stored (the elastic portion). The out-of-phase component of *E**, i.e. the shear loss modulus E'', represents viscous component of it. The complex dynamic shear viscosity η* can be obtained from *E** divided by the frequency, while the dynamic viscosity is $\eta = E'' / \omega$.

3.1.2 Temperature dependence of the relaxation time

The temperature dependency of polymer properties is of great importance because the physical and mechanical properties of the polymers change drastically as temperature changes. It is important to study the relaxation behavior of polymers, at a particular temperature for a given time period. The temperature dependency of the relaxation time provides a way of varying the temperature to bring the relaxation process within a time scale that is readily accessible. Viscoelastic behavior at short or long time periods can be predicted by extrapolation. Changes due to temperature can be described in terms of free volume or relaxation time. At temperatures below $T_{g,}$ local chain relaxation takes place. At these temperatures motions are hindered by close presence of other molecules. For relaxation to take place a potential barrier must be surmounted. In this region the kinetics of relaxation are better described on the basis of barrier state theories; as such the temperature dependency of the relaxation time τ is often described by the Arrhenius equation (Sperling, 1992; Fried, 1995).

$$\tau = \tau_o \exp\left[\frac{E_a}{kT}\right] \tag{3.16}$$

where τ_o is the pre-exponential factor, E_a is the activation energy, k is Boltzmann constant and T is the absolute temperature.

In contrast to local motions, relaxation times τ associated with secondary motions are dependent on free volume. The presence of volume allows the molecules to relax to a new configuration. The Doolittle equation gives a relation that expresses the dependency of relaxation time on the free volume (Doolittle and Doolittle, 1957).

$$\tau = \tau_o \exp\left(\frac{BV_O}{V - V_O}\right) \tag{3.17}$$

where V is the total volume, V_0 is the occupied volume, $B = \xi\left(\frac{V^*}{V_m}\right)$ is a constant, V^* is the minimum volume required for relaxation process to take place, V_m is the mean volume of the relaxing polymer segment, ξ is a constant such that $0.5 < \xi < 1$.

At temperature above the glass transition (T_g), the dependency follows the William-Landel-Ferry (WLF) law (Hadley and Ward, 1993),

$$\log \frac{\tau(T)}{\tau(T_g)} = -\frac{C_1(T - T_g)}{C_2 + T - T_g} \tag{3.18}$$

where $\tau(T)/\tau(T_g)$ is the shift factor relative to the reference temperature, $T_{g..}$ For temperatures less than the reference temperature the shift factor shifts the curves to the right while for higher temperatures to the left. C1 & C2 are empirically determined constants, T is the selected temperature, in °C or K, and T_g is the reference temperature, in °C or K, which is a glass transition temperature. The values of C1 and C2 depend on the particular morphology or structure associated with a given sample. For amorphous materials, the best approximations for the parameters are C_1 = 17.44 and C_2 = 55.6. As the sample becomes more crystalline (e.g. polyethylene or the asphalt paraffins) or cross linked (such as a vulcanized rubber), the values of C_1 and C_2 will increase, reflecting changes in the free volume and the expansion with respect to temperature. Conversely, Vogel-Fulcher-Tamman (Vogel *et al.*, 1921) equation can also be used to explain temperature dependency above T_g.

$$\tau = \tau_o \exp\left[\frac{K}{T - T_o}\right] \tag{3.19}$$

Where τ_o is the characteristic time at which free volume would be zero, $K = \left(\frac{BV_O}{\alpha}\right)$ is a constant and T_o is ideal (Vogel) temperature which is 50 ^oC below T_g, or temperature at which free volume would be zero.

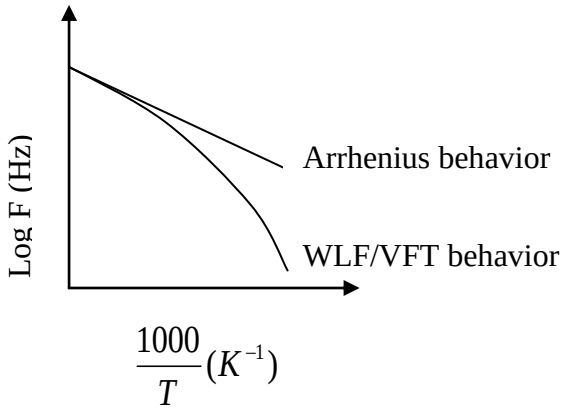

Figure 3.4: Comparison of the Arrhenious and VFT/WLF relationship.

From the figure 3.4 above, it can be seen that at high temperatures the two are approximately the same but differ significantly at lower temperatures.

3.2 Creep and recovery behavior

Creep is the tendency of a solid material to slowly move or deform permanently under the influence of stresses. It occurs as a result of long term exposure to high levels of stress that are below the yield strength of the material. Creep is more severe in materials that are subjected to heat for long periods, and near melting point. Creep always increases with temperature. The rate of this deformation is a function of the material properties, exposure time, exposure temperature and the applied structural load. Depending on the magnitude of the applied stress and its duration, the deformation may become so large

that a component can no longer perform its function. The general creep equation [Rosato, 2001] is;

$$\frac{d\varepsilon}{dt} = \frac{C\sigma^m}{d^b} e \frac{-E_a}{KT} \tag{3.20}$$

where ε is the creep strain, *C* is a constant dependent on the material and the particular creep mechanism, *m* and *b* are exponents dependent on the creep mechanism, E_a is the activation energy of the creep mechanism, σ is the applied stress, *d* is the grain size of the material, *k* is Boltzmann's constant, and *T* is the absolute temperature.

3.2.1 Creep stages

When a load is applied to material, an instantaneous deformation occurs as pure elastic response. The deformation is followed by a rapidly decreasing deformation called primary deformation. This is followed by a steady state linear deformation called secondary deformation. As the sample approaches failure the deformation accelerates until fracture; which is called tertiary deformation. A typical creep curve is represented in figure 3.5.

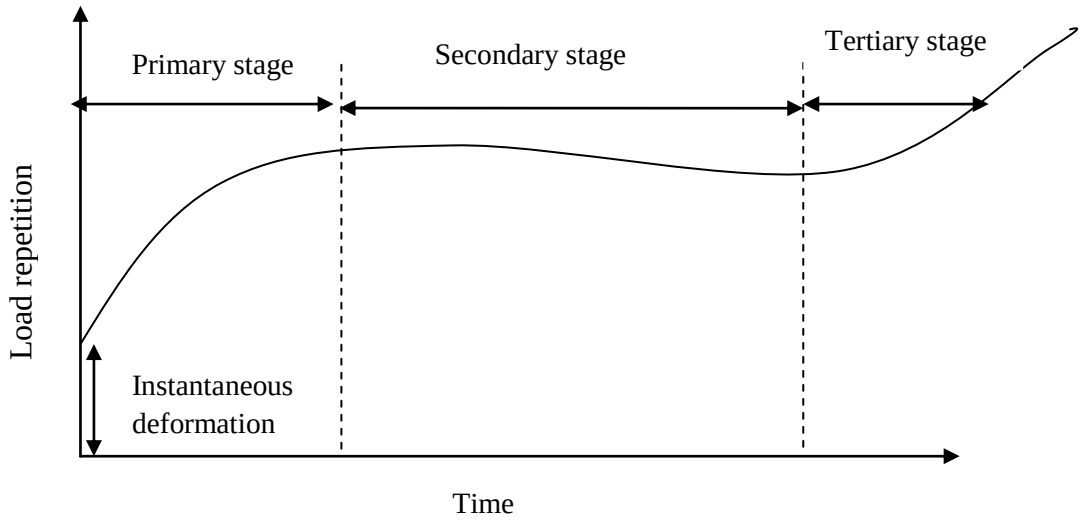

Figure 3.5: Typical creep curve.

Instantaneous deformation: under the application of an initial and relatively small load, a material behaves as elastic. There occurs a sudden deformation as soon as the initial load is applied. The strains are fully recoverable, which can be explained by the behavior of a Hookean spring. In other words, no permanent strain is generated during a loading and unloading cycle.

Primary stage: During this stage, creep proceeds at a diminishing rate due to work hardening. If the load is continuously applied, the material continues to deform with a decreasing rate. In other words, the permanent strain rate slows down with time. The deformation characteristic can be simply explained by the Kelvin model. The behavior is that after unloading the material, a part of deformation is recoverable. The physical damage process during the primary stage is called strain hardening. This results in increase in the plastic strain. On the contrary, the dislocation intersections decrease the movement in the body which causes a permanent strain rate reduction.

Secondary stage: This stage proceeds at a constant rate because a balance is achieved between work hardening and annealing (thermal softening) processes. Secondary creep, also known as steady-state creep is initialized by micro-cracks. Microcracking is the damage process during the secondary stage. At this point where microcracking initiates the decrease in the permanent strain ends. During this stage, slope deformation is nearly linear, at this stage, the strain rate eventually reaches minimum and becomes nearly a constant. The stress dependency of this rate is related to the creep mechanism. The deformation that accumulates at this stage is unrecoverable.

Tertiary stage: the permanent deformation rate starts to increase, and rapidly accumulates during this stage. The creep rate increases due to necking and the associated increase in local stress of the specimen. Continuous loading initiates macrocracking hence increased deformation rate. This stage represents the plastic failure of the material.

Creep behavior of polymers also depends heavily on the material temperature during testing and has the highest rate of deformation around the glass transition temperature. A polymer at a specific temperature and molecular weight may behave as a liquid or a solid depending on the time scale at which its molecules are deformed. This behavior is generally referred to as viscoelastic behavior. In cross-linked polymers, the cross-linking acts to decrease the viscous component of viscoelastic behavior as the chains are prevented from slipping past one another. Linear viscoelastic theory can be applied to polymers when stress (or strain) are low. Linear elastic fracture mechanics approach has also shown considerable promise in correlating non-linear behavior of polymers and non –linear models being developed (Osswald and Menges, 2003). The extent of deformation also depends on size of the load, time, structure and morphology of the polymer (Painter and Coleman, 1994). Temperature and biopolymers such starch and cellulose affects the stiffness of HDPE, the stiffness decreases with increase in the temperature. The frequency of load, short pulse periods cause higher cumulative permanent strain in the repeated load creep tests, that is, higher loading rates increases the permanent strain.

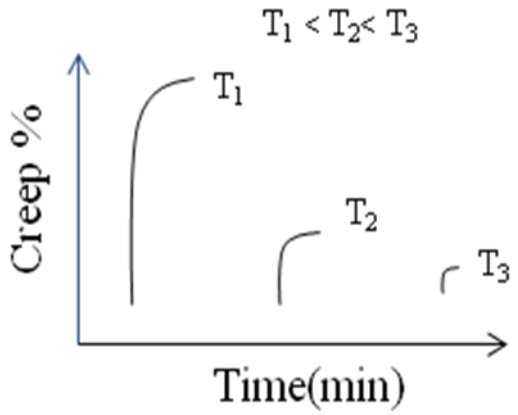

Figure 3.6: creep strain % versus time at constant load as a function of temperature.

Various models have been proposed to explain viscoelastic behavior. The spring element shows instantaneous elasticity due to loading and recovery due to unloading. This model fits well to purely elastic materials. Spring, which represent the elastic component of a viscoelastic material, obey Hooke's Law:

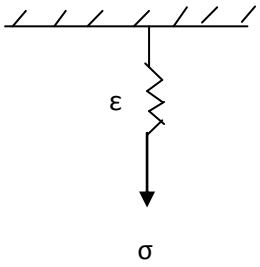

Figure 3.7: Linear spring-Elastic component

The constitutive equation for this element is;

$$\sigma_s = E\varepsilon \tag{3.21}$$

where σ is the applied stress, E is the creep modulus of the material, and ε is the strain. The spring represents the energetic or elastic component of the model's response. The time dependency of viscoelastic materials are generally modeled with linear viscous

dashpot. The dashpot continuously deform at a constant rate when constant stress is applied. The dashpot represents the viscous component of a viscoelastic material. In these elements, the applied stress varies with the time rate of change of the strain:

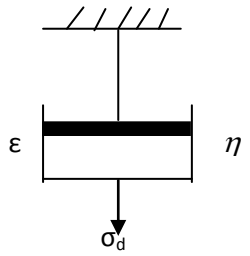

Figure 3.8: Linear dashpot-Viscous component.

The constitutive equation of this element is;

$$\sigma_d = \eta \frac{d\varepsilon}{dt} \tag{3.22}$$

where η; is viscosity of the dashpot component.

Several mathematical models have been developed to describe the nature of viscoelastic materials using a spring and dashpot. These include Kelvin-Voigt, Maxwell, Burgers and standard linear solid models, among others (Sperling, 1992; Fried, 1995; Williams, 1998).

3.2.2 Kelvin-voigt model

The Kelvin–Voigt model, also called the Voigt model, can be represented by a purely viscous damper and purely elastic spring connected in parallel as shown in figure 3.9 below. A viscous material is modeled as a spring and a dashpot in series with each other,

both of which are in parallel with a lone spring.

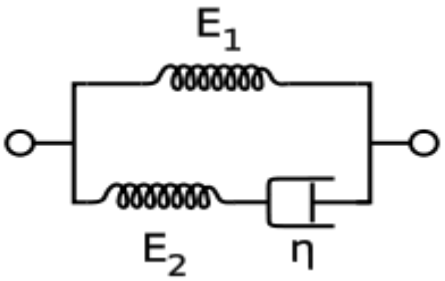

Figure 3.9: Schematic representation of the Kevin-Voigt model.

For this model, the governing constitutive relation is:

$$\frac{d\varepsilon}{dt} = \frac{\frac{E_2}{\eta}\left(\frac{\eta}{E_2}\frac{d\sigma}{dt} + \sigma - E_1\varepsilon\right)}{E_1 + E_2} \tag{3.23}$$

Under a constant stress, the modeled material will instantaneously deform to some strain, which is the elastic portion of the strain, and after that it will continue to deform and asymptotically approach a steady-state strain. This last portion is the viscous part of the strain. The creep strain is given by;

$$\varepsilon(t) = \sigma C_0 + \sigma C \int_0^\infty f(\tau)(1 - \exp[-t/\tau])\, d\tau \tag{3.24}$$

where: σ is the applied stress, C_0 is the instantaneous creep compliance C is the creep compliance coefficient τ is the retardation time and $f(\tau)$ is the distribution of retardation times.

When at a time t_o, a viscoelastic material is loaded with a constant stress that is maintained for a sufficiently long time period (figure 3.10), the material responds to the stress with a strain that increases until the material ultimately fails. When the stress is maintained for a shorter time period, the material undergoes an initial strain, ε_o until a time t_1 at which the stress is relieved, at which time the strain immediately decreases (discontinuity) then continues decreasing gradually to a residual strain.

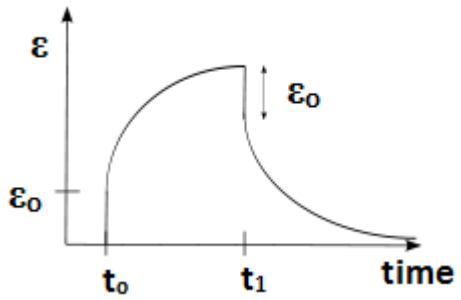

Figure 3.10: Creep strain and recovery as a function of time.

3.2.3 Maxwell model

The Maxwell model can be represented by a purely viscous damper and a purely elastic spring connected in series, as shown in figure 3.11.

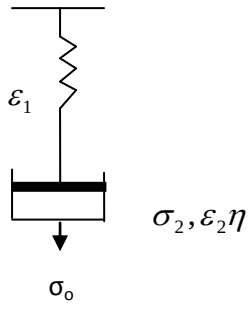

Figure 3.11: Maxwell model.

The total stress, σ_T and the total strain, ε_T can be defined as follows:

$$\sigma_T = \sigma_1 = \sigma_2 \tag{3.25}$$

$$\varepsilon_T = \varepsilon_1 + \varepsilon_2 \tag{3.26}$$

In this model, stress σ, strain ε and their rates of change with respect to time *t* are governed by equations of the form:

$$\frac{d\varepsilon}{dt} = \frac{\sigma}{\eta} + \frac{1}{E}\frac{d\sigma}{dt} \tag{3.27}$$

where E is the elastic modulus and η is the material coefficient of viscosity. If a Maxwell material is suddenly subjected to a stress σ_o, then the elastic element would suddenly deform and the viscous element would deform with a constant rate:

$$\varepsilon(t) = \frac{\sigma_o}{E} + \frac{\sigma_o}{\eta}t \tag{3.28}$$

The Maxwell Model is not ideal for predicting the creep behavior of a material since it describes the strain relationship with time as linear.

3.2.4 Burgers model

It combines Maxwell model in series with a certain number of Kelvin-voigt models as shown in figure 3.12a. It is one of the most used models to give the relationship between the morphology of the blends and their creep behavior (Findley *et al*., 2007). For linear viscoelastic solid, the total strain is the sum of three essentially separate parts: the immediate elastic deformation, the delayed elastic deformation and the Newtonian flow, which is identical with the deformation of a viscous liquid obeying Newton's law of viscosity.

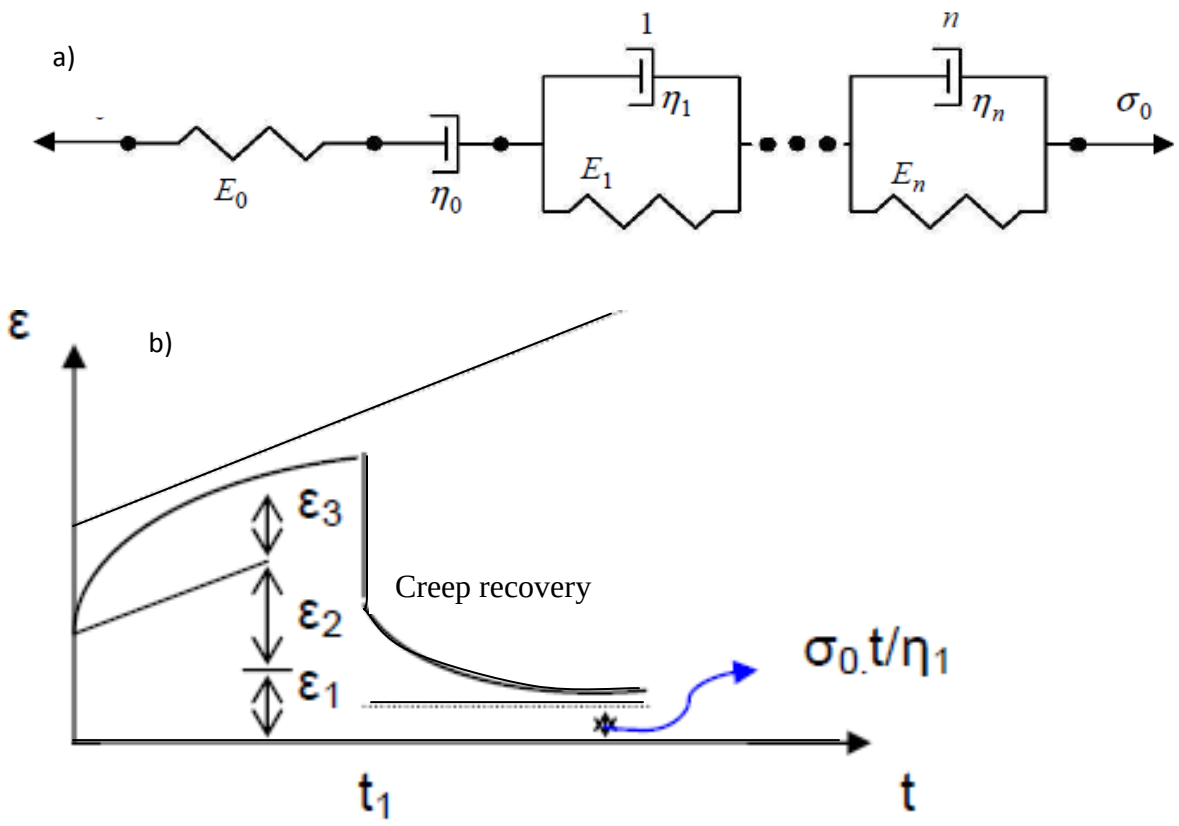

Figure 3.12: a) Generalized Burgers Model, (b) creep and recovery.

For linear viscoelastic solid, the total creep strain ε_T is given by the Burgees model; which is a series combination of the Maxwell and Kelvin – Voight models.

$$\varepsilon_T = \varepsilon_1 - \varepsilon_2 - \varepsilon_3 = \frac{\sigma}{E_1} - \frac{\sigma}{E_2}[1 - \exp(-E_2/\eta_2) - \sigma t/\eta_3] \qquad (3.29)$$

where ε_1 is the instantaneous elastic deformation, ε_2 is the delayed elastic deformation and ε_3 is the Newtonian flow, which is identical to the deformation of viscous liquid obeying Newton's Law of viscosity. E_1 and E_2 are elastic moduli, η_1 and η_2 are viscosities, σ is the applied stress, and t is the creep time.

If a constant stress is applied to the extremities of the mechanical model, because of the equilibrium, the same stress is shared by each element while the strains (and stress rates) are added up giving;

$$\varepsilon(t) = \sigma\left[\frac{1}{E_o} + \frac{1}{\eta_o} + \sum_{i=1}^{n}\frac{1}{E_i}\left(1 - e^{\frac{t}{\tau_i}}\right)\right] \tag{3.30}$$

As can be seen, parameters are necessary for completely describing the generalized burgers model, namely $E_{o,}\ \eta_o$, E_i and $\tau_i = \eta_i / E_i$ (i = 1,2,3….), which are, respectively, the instantaneous elastic modulus, the viscosity of the Maxwell element, delayed elastic modulus and the relaxation time of the generic i-th voigt element. The strain per unit of applied stress provides the so called creep compliance, from equation (3.28), we recognize that the generalized burgers model provides an exponential decay of the creep compliance. This is not surprising because in this model spring and dashpot yield forces that are proportional to derivatives of zero-th order (spring) and first order (dashpot).

3.2.5 Standard linear solid model

The standard linear model combines a spring and a Kelvin element in series as shown in figure 3.13.

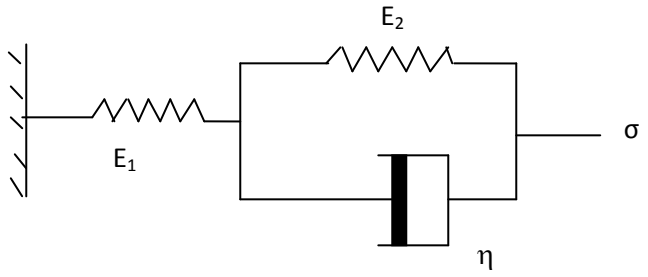

Figure 3.13: Standard linear solid model.

By considering equilibrium of stress and compatibility of strains, the governing equation for this model is:

$$\eta E_1 \frac{d\varepsilon}{dt} + E_1 E_2 \varepsilon = \eta \frac{d\sigma}{dt} + (E_1 + E_2)\sigma \tag{3.31}$$

For a constant stress $\sigma_{o,}$ the corresponding strain is obtained by solving equation (3.31). Since stress is a constant, $\frac{d\sigma}{dt} = 0$, and equation (3.31) becomes,

$$\eta E_1 \frac{d\varepsilon}{dt} + E_1 E_2 \varepsilon = (E_1 + E_2)\sigma \tag{3.32}$$

This can be rewritten as,

$$\frac{d\varepsilon}{dt} + \frac{E_2 \varepsilon}{\eta} = (E_1 + E_2)\frac{\sigma}{\eta E_1} \tag{3.33}$$

Noting that the equation has an integrating factor, $e^{\frac{E_2 t}{\eta}}$, we obtain an expression for strain as;

$$\varepsilon e^{\frac{E_2 t}{\eta}} = (E_1 + E_2)\frac{\sigma}{E_1 E_2} e^{\frac{E_2 t}{\eta}} + C \tag{3.34}$$

At t = 0, $\varepsilon = \frac{\sigma_0}{E_1} + \frac{\sigma_o}{E_2}$ substituting these values in (3.34) and solving for C, we obtain an expression of strain as;

$$\varepsilon = \frac{\sigma_0}{E_1} + \frac{\sigma_0}{E_2}\left[1 - \exp\left(-\frac{t}{\tau}\right)\right] \tag{3.35}$$

where; $\frac{\sigma_0}{E_1}$ is instantaneous elastic deformation corresponding to the spring $\frac{\sigma_0}{E_2}$ is delayed elastic deformation corresponding to the Kelvin element, E_1 and E_2 are elastic moduli. At t =0, $\varepsilon = \frac{\sigma_o}{E_1}$ and $\tau = \frac{\eta}{E_2}$, where η is viscosity, τ is retardation (relaxation) time, which is defined as the time take for the stress to fall to a value $\frac{1}{e} = \frac{1}{2.7}$ of the original stress. In other words it is the measure of how quickly a material recovers. This is shown in figure 3.14.

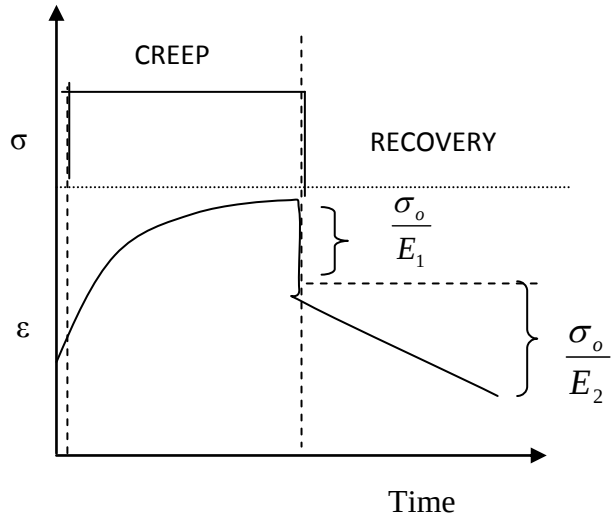

Figure 3.14: Creep response of standard linear solid model.

The time dependences of the relaxed moduli in the creep (C_p) and subsequent recovery (R) processes at different loading levels are given by;

$$C_p = \frac{E_0 - E_t}{E_0} \text{ and } R = \frac{E_0^{'} - E_t^{'}}{E^{'}_0} \tag{3.36}$$

where; E_t represents the creep modulus at time t seconds, E'_t represents the modulus at the time t in the recovery process, E_o represents the original modulus in the creep process, E'_o is the initial modulus in the subsequent strain recovery process at 10 s after 3600 s of creep. This work has adopted the standard linear solid model, because the model provides a good qualitative description of both creep and stress relaxation behavior of polymeric materials. The responses of this model, under both creep and stress relaxation conditions were analyzed. In this model, at any point in time, stress is directly proportional to the strain.

3.3 Diffusion behavior

Transport of gases, vapors and liquids through polymer blends is an important and in some cases a controlling factor in several applications such as protective coatings, membrane separation processes and packaging of foods and beverages. The transports of small molecules through polymer membranes occur due to random molecular motion of individual molecules (Chainley, 1989). This process tries to equalize the concentration difference or the chemical potential of the penetrant in the phases separated by the membranes. This process can be described in terms of Fick's first law of diffusion according to which the flux J, in the direction of flow is proportional to the concentration gradient , $\frac{\partial C}{\partial x}$ as;

$$J = - D \frac{\partial C}{\partial x} \qquad (3.37)$$

where, D is the concentration gradient at steady rate. On the other hand, Fick's second law describes non steady state for transport process, which is given by the rate of change of the concentration $\frac{\partial C}{\partial x}$, at a plane within the membrane;

$$C\ \frac{\partial C}{\partial t} = \frac{D\partial^2 C}{\partial x^2} \tag{3.38}$$

This is an ideal case in which the membrane is isotropic and diffusion coefficient is independent of distance, time and concentration. Transport behavior in polymers depends on polymer nature (e.g. polymer weight), nature of crosslinks, effect of plasticizers, nature of penetrant, fillers and temperature (Mears, 1954). The total amount of substance diffusing in the polymeric material (M) as a function of time is given by the integral of equation 3.38 across the thickness (h):

$$\frac{M_t}{M_{\max}} = 1 - \frac{8}{\pi^2}\sum_{n=0}^{\infty}\frac{1}{(2n-1)^2}\exp[-D(2n+1)^2\pi^2\, t/h^2] \tag{3.39}$$

where, M_{max} is the maximum quantity of the diffusing substance at infinite time. A simplified form of equation 3.39 for values of $M/M_{\max}$ lower than 0.6 (Crank, 1975) has the form;

$$\frac{M_t}{M_{\max}} = \frac{4}{h\sqrt{\pi}}\sqrt{Dt} \tag{3.40}$$

For polymer analysis equation 3.40 is a valid representation of the Fickian diffusion behavior in a material which can be confirmed if the following characteristics are observed:

a) Both uptake and desorption plots of M_t/M_{max} versus $t^{1/2}$ are initially linear.

b) The linear region extends to at least M_t/M_{max}=0.6.

c) Above the linear region, the curves are concave against the abscissa.

3.4 Thermal degradation

Under normal conditions, photochemical and thermal degradation are similar and are classified as oxidative degradation. The difference between the two is that thermal reactions occur throughout the bulk of the polymer sample, whereas photo-chemical reactions occur on the surface (Tayler, 2004). Thermal degradation is a process whereby the action of heat or elevated temperatures on a material, product or assembly causes a loss of physical, mechanical or electrical properties. At higher temperatures, the components of the long chain backbone of the polymer begin to separate (molecular scission) and react with one another to change the properties of the polymer. The typical properties that change include: reduced ductility and embrittlement, chalking, color changes and cracking (Villetti and Parasama, 2002). It is studied using Thermo-gravimetric analysis (TGA) which can be used for investigation of oxidative and thermal degradation of the polymers (Anthony, 1999). Mass loss for the polymer up to 550 ºC was observed and degradation investigated.

The TGA profiles of HDPE/ CELL and inoculated blends made by mechanical blending were shown. Mass loss for the polymer up to 550 ºC was observed and degradation investigated. When a polymer sample degrades, its mass decreases due to production of gaseous products like carbon IV oxide, carbon (II) oxide and water vapor. The rate of

degradation in TGA ($d\alpha/dt$) is defined as the rate of change of the degree of conversion. The degree of conversion is given by:

$$\alpha = (W_o - W)/(W_o - W_\infty) \quad (3.41)$$

where, Wo, W and W∞ are the initial weight, the actual weight at each point of the curve, and the final weight measured at the end of degradation process, respectively.

3.4.1 Mechanism of HDPE thermal degradation

HDPE thermal degradation is a radical chain mechanism involving three major stages: Stage one is the initiation of thermal degradation which involves the loss of a hydrogen atom from the polymer chain when the polymer absorbs heat or light. This creates a highly reactive and unstable polymer "free radical" (R*) and a hydrogen atom with an unpaired electron (H*). The strength of the C-F bond means that there it is much harder for thermal degradation to initiate. Secondly, is the the propagation stage of thermal degradation which involves a variety of reactions and one of these is where the free radical (R*) reacts with an oxygen (O_2) molecule to form a peroxy radical (ROO*) which can then remove a hydrogen atom from another polymer chain to form a hydroperoxide (ROOH) and so regenerate the free radical (R*). The hydroperoxide can then split into two new free radicals, (RO*) + (*OH), which will continue to propagate the reaction to other polymer molecules. The process can therefore accelerate depending on how easy it is to remove the hydrogen from the polymer chain. Last stage is the termination of thermal degradation which is achieved by "mopping up" the free radicals to create inert products. This can occur naturally by combining free radicals or it can be assisted by

using stabilizers in the plastic. A general mechanism for thermal degradation is shown below.

X* = free radical

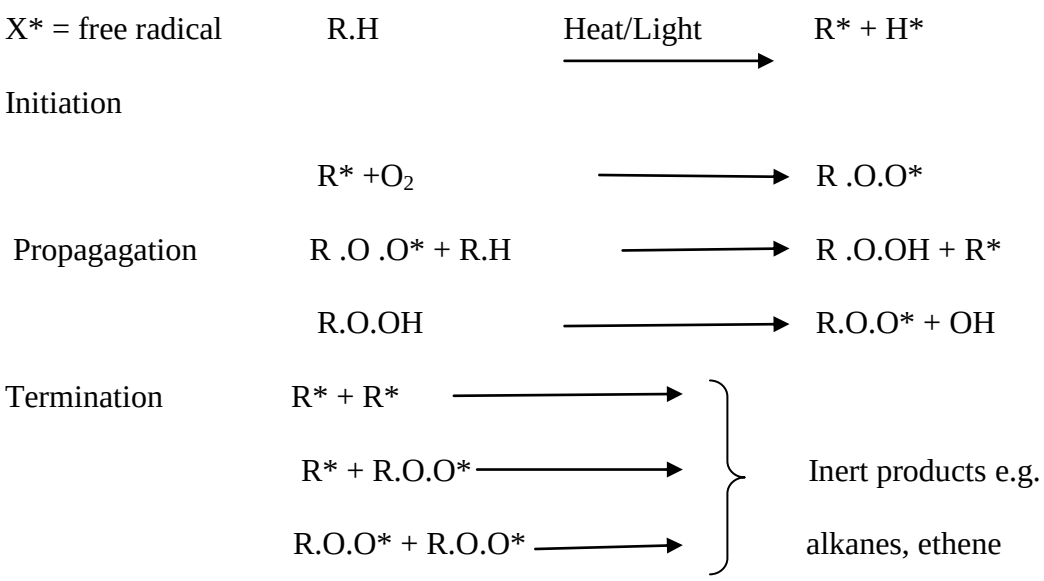

3.4.2 Mechanism of cellulose thermal decomposition

Decomposition of cellulose involves at least four processes in addition to simple desorption of physically bound water. The first is the cross-linking of cellulose chain, with the evolution of water (dehydration). The second concurrent reaction is the unzipping of the cellulose chain (transglycosidation). Laevoglucosan is formed from the monomer unit. The third reaction is the decomposition of the dehydrated product (dehydrocellulose) to yield char and volatile products. Finally the laevoglucocosan can further decompose to yield smaller volatile products, including tars and eventually, carbon monoxide (Brauman, 1988).

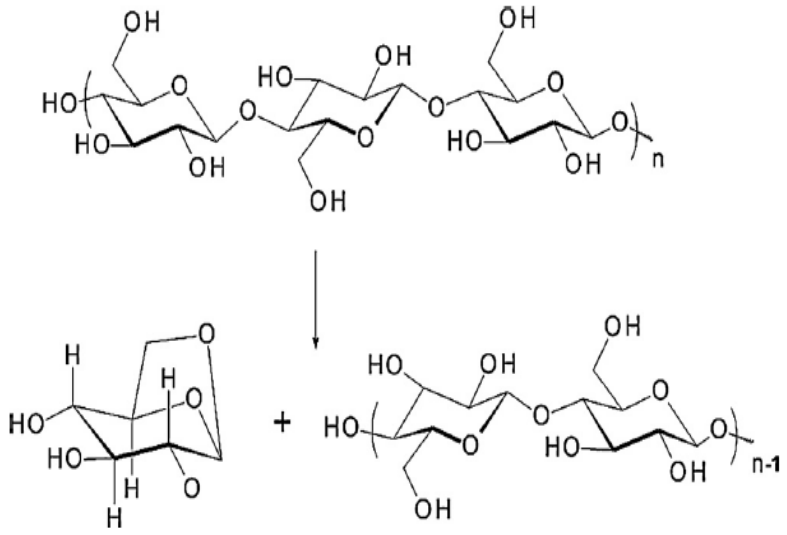

Figure 3.15: Formation of Levoglucosan through unzipping of the cellulose chain.

(Lomankin *et al*., 2011).

3.4.3 Activation energy

The most commonly used approaches to evaluate kinetic parameters is first to measure mass loss behavior of the material during decomposition and then apply various equations to fit the experimental data. The activation energies for the decomposition of the blends are important in assessing the reaction mechanisms (Grija *et al*., 2005).

3.4.3.1 Arrhenius model

The Arrhenius relationship is given by equation 3.42;

$$ln\left(\frac{dx}{dt}\right) = ln\, A + \mathrm{n}(1 - x) - \frac{E_a}{RT} \qquad (3.42)$$

where, x is the fractional conversion, A is the frequency factor and E_a is the activation energy. The parameters, R, T and n represent the universal gas constant, temperature in Kelvin and the order of reaction, respectively. For non-isothermal data obtained at a constant heating rate $\beta = dT/dt$, equation (3.42) can be rewritten as:

$$\ln \beta = \ln \left(\frac{A(1-x)^n}{(dx/dT)} \right) - \frac{E_a}{RT} \tag{3.43}$$

The slope of a graph of ln β versus 1/T can be used to ascertain E_a of a material.

3.4.3.2 Broido model

The Broido method (Broido, 1969) has been used to evaluate the kinetic analysis of the main thermal decomposition process of materials. The equation is given as:

$$\ln \ln \left(\frac{1}{x} \right) \cong -\frac{E_a}{RT} + \ln \left(\frac{RZ}{\beta T^2{}_{Max}} \right) \tag{3.44}$$

where R is the gas constant, T is the absolute temperature, E_a is the activation energy, Z is the frequency factor, β is the heating rate, T^2_{Max} is the temperature of maximum reaction rate and x is the residual fraction calculated as;

$$X = \frac{w - w_\infty}{w_0 - w_\infty} \tag{3.45}$$

where w_0 is the initial mass, w is the sample mass at time t and w_∞ is the final mass.

Testing of polymers for thermal stability is done by accelerated test method which involves increasing temperatures over short times and the results are then extrapolated back to the lower service temperature and longer time of the real application. This research assumed a mechanism based on Broido model.

CHAPTER FOUR

MATERIALS AND METHODS

4.1 Materials

The materials that were used in this study are high density polyethylene (HDPE) - grade (HD6605) with a melt index of 0.005Kg/10min (190 °C, 2.16 Kg) and a density of 948 Kg/m^3, cellulose and spores of *Aspergillus niger* fungus. The high density polyethylene pellets were obtained from a plastic company in Nairobi while cellulose was obtained from the cell sap of acacia tree at Kenyatta University. Some of the typical properties of high density polyethylene and cellulose are shown in the Table 4.1.

Table 4.1: Typical properties of HDPE and cellulose.

Property	**HDPE (range)**	**Cellulose**	**Reference**
Melting temperature, T_m (K)	400-408	_	Van, 1990
Molecular structure	$(-CH_2-)$ n	$(C_6H_{10}O_5)$ n	Sperling,1992
Molecular weight, (g/mole)	150,000-500,000	_	Sperling,1992
Crystallinity (%)	80-95	_	Van, 1990
Tensile strength, (Mpa)	21-38	17.8	Van, 1990
Tensile modulus, (Gpa)	0.14-1.24	_	Van, 1990
Glass transition, T_g (K)	140-180	Decompose	Van, 1990

The strain of *Aspergillus niger* was isolated from a damp. Identification of the strain was carried out at the Plants and Microbial Science Department of Kenyatta University. The

fungus was then incubated at 30 °C for two weeks to form a culture then spores harvested.

4.1.1 Sample molding apparatus

The sample molding apparatus consisted of a brass cylindrical heating chamber. It had dimensions of; length of 40 mm and diameter 10 mm (figure 4.1a). It was open on one side and closed on the other side with a 2 mm diameter hole for passage of polymer melt. A stopper screw was used to close the hole during heating and removed just before the melt was injected. The system also included a 3 mm thick steel heating /molding tray (figure 4.1b) of dimensions about; length 50 mm, width 28 mm and height 25 mm and a cuboid cover about 24 mm length, 8.8 mm width 3 mm thick that was used to cover the tray while hot pressing.

(a)

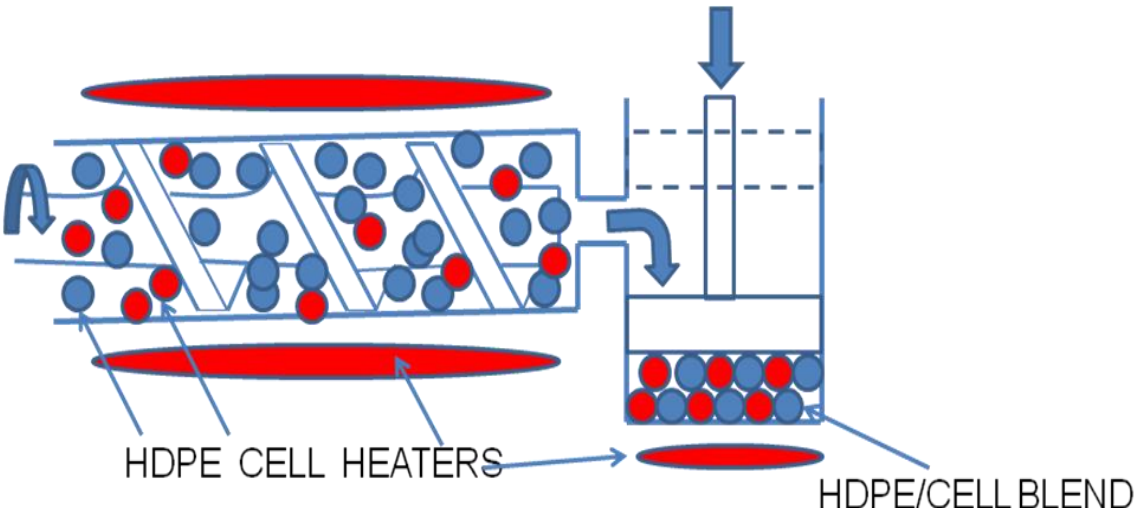

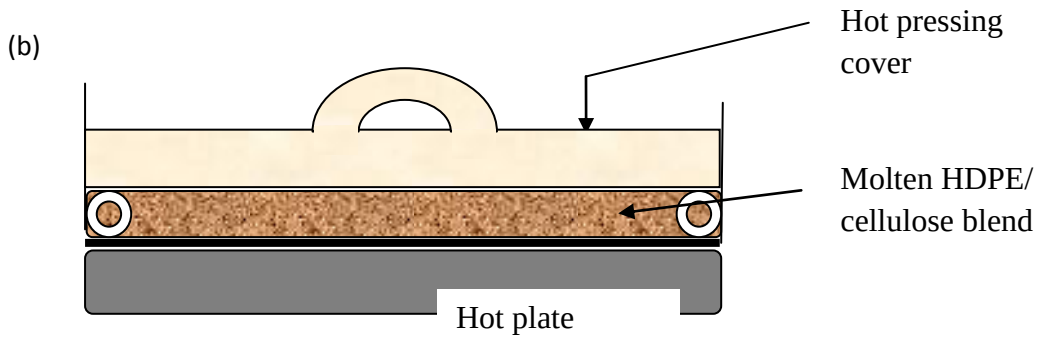

Figure 4.1: Hot pressing Apparatus; (a) Heating chamber and molding tray (b) two dimensional look of the system.

4.2 Sample preparation

A total mass of 8 g was used as reference mass to determine the proportions of HDPE and cellulose in the blend. Cellulose concentrations were increased in steps of 5 % starting with 0 %. The masses of HDPE and cellulose as well as their respective percentage concentrations are shown in Table 4.2.

Table 4.2: Masses of HDPE and cellulose as well as their % concentrations**.**

MASS (g)		MASS CONCENTRATIONS (%)	
HDPE	Cellulose	HDPE	Cellulose
8	0	100	0
7.6	0.4	95	5
7.2	0.8	90	10
6.8	1.2	85	15
6.4	1.6	80	20
6.0	2	75	25
5.6	2.4	70	30

Cellulose from Acacia cell sap was dried at about 90 ^{o}C and crushed using a mortar and pestle into a fine powder. The powder was then sieved to remove any debris. Appropriate quantities of HDPE granules were then heated to 150 ^{o}C for about 10 minutes in the heating chamber (figure 4.1a). Molten HDPE was then mixed with crushed cellulose in the mass percentage ratios as shown in Table 4.2. During mixing a stirrer fitted to a motor with a variable rotation speed up to about 240 rotations per minute was used. By varying the voltage across it, the appropriate speed was set and used to achieve a homogeneous blend. Once heated, spacers were dropped at the edge of the molding chamber and the blend covered with the hot cover (figure 4.1b). The heating boat was then removed from

the heating plate and pressed vertically down to the level of the spacers. The mold was then allowed to cool for 10 minutes to form a block. From the block two samples were cut as illustrated in figure 4.2. The dimensions of the cut samples were 25 mm x 4 mm x 3 mm.

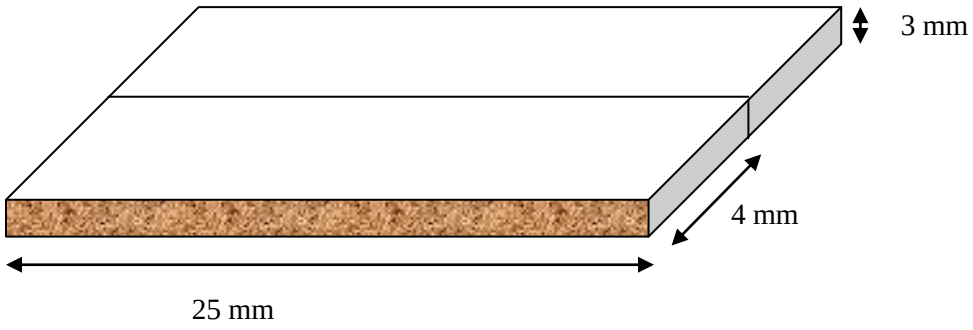

Figure 4.2: Sample dimensions**.**

4.2.1 Sample inoculation

Seven, 250 ml conical flasks were washed thoroughly, rinsed in distilled water and dried at room temperature. Sterilization of the flasks was done in aseptically sterilized steam autoclave machine at a pressure of 15 psi and a temperature of 121 ^{o}C for 30 minutes. 50 g of potato dextrose agar was dissolved in 1.05 litres of distilled water in a 5 litre flask as per the manufacturers' instructions. A suspension of potato dextrose agar (PDA) was prepared and equal amounts (150 ml) sub-divided into seven conical flasks. The PDA in the flasks was allowed to cool in order to solidify. A strain of *Aspergillus Niger* was then dropped on top of the PDA in the sterile laminar flow safety hood. Pre-weighed samples of HDPE/CELL were then put in conical flasks containing pure active *Aspergillus niger* culture. The flasks were closed using aluminium foil to avoid any kind of contamination and then incubated at 30 °C for 60 days. The only carbon source for the growth of the fungus was from the samples.

After exposing to fungal isolates for 2 months, HDPE/CELL were harvested, washed in ethanol to remove all fungal traces, air- dried overnight at room temperature and equilibrated and then weights determined. The cultured samples were then compared to uncultured samples. The recovered plastic samples were then analyzed for biodegradation by weight loss before and after microbial treatment using an electronic balance. The percentage weight loss of the inoculated HDPE/CELL samples was calculated from the formula;

$$\%\ weight\ loss = \frac{Initial\ weight\ -\ Final\ weight}{Initial\ weight} \qquad (4.1)$$

4.3 Measurements

4.3.1 Dynamic mechanical analysis

Dynamic mechanical testing of the properties of HDPE/CELL blends were determined using DMA2980 TA instrument. The shape of the test sample was a rectangular strip of dimensions (17.93 mm × 12.62 mm × 3.17 mm). The single cantilever mode of deformation was used under the test temperature from -30 °C to 120 °C at a heating rate of 5 °C/min. Storage modulus E' and loss modulus E'' of each sample were recorded in a multi-frequency mode at 1 Hz, 3 Hz, 5 Hz, 10 Hz, 15 Hz, 20 Hz, and 30 Hz.

4.3.2 Creep measurement

Creep and recovery behavior of both the inoculated un-inoculated HDPE/CELL blend samples were investigated using DMA 2980 in single cantilever mode with a constant time span of 12 minutes. A sample was placed on the bottom support and the top probe was adjusted to touch it. The oven was set to a desired temperature and allowed to

equilibrate for 10 minutes. Then a contact pressure of 100 Pa was placed on the sample. Creep measurements were done by applying stresses of 0.03, 0.07 and 0.02 Mpa respectively at 30 °C, 40 °C, 50 ^{o}C and 60 °C. Time span for application of force was 12 minutes and so to the recovery time.

4.3.3 Water absorption test

This test was carried out to study the water resistance in both inoculated and un-inoculated HDPE/CELL blends. All the samples were dried at 80 °C in a vacuum oven for 3 hours, cooled in a desiccator and immediately weighed to the nearest 0.001 g. Each sample was placed in a conical flask containing 10 ml of distilled water maintained at room temperature. The flasks were firmly covered by aluminium foil to prevent entry of moisture. The samples were then removed weekly from the water one at a time, gently blotted with tissue paper to remove the excess water on the surface, weighed to the nearest ± 0.001 g immediately and returned in the water. The weighings were repeated at the end of every week for 6 weeks and values recorded. Percentage increase in weight during immersion was calculated to the nearest 0.01 %.

4.3.4 Thermal degradation

Thermal-gravimetric analysis (TGA) was used to determine the degradation temperature of the samples. Both un-inoculated and inoculated HDPE/CELL blend samples were scanned using Lindiberg Blue Tube Furnace (TF55035c-1) within a temperature range of 25 °C-550 °C at a heating rate of 5 °C/minute. The mass of the samples was measured using a sensitive balance and the initial mass of each blend was 10 mg. The process was carried out in an oxidative environment.

CHAPTER FIVE

RESULTS AND DISCUSSIONS

5.1 Introduction

This chapter gives an insight of the experimental results of diffusion, TGA, and DMA. Central to the discussion, is the effect of CELL and inoculation by *Aspergillus niger* on the diffusion, thermal, and mechanical properties of HDPE/CELL blends.

5.2 Diffusion test

The water absorption capacity and the biodegradability are the most important properties for biodegradable materials. Water absorption is an important parameter for any polymer particularly for cellulose and starch blends since they are hydrophilic polymers. Biopolymers such as starch and cellulose influences the water absorption of HDPE/CELL blends.

5.2.1 Effect of cellulose on water uptake

The water uptake phenomenon can be observed through figure 5.1 which shows that water uptake of the HDPE/CELL blends increased with CELL content and immersion time. Thus, in agreement with that reported by (Bhattacharya and Mani, 1998), Danjaji *et al*. (2002) and Mali *et al*. (2005) that moisture uptake increased with immersion time and increasing filler concentrations.

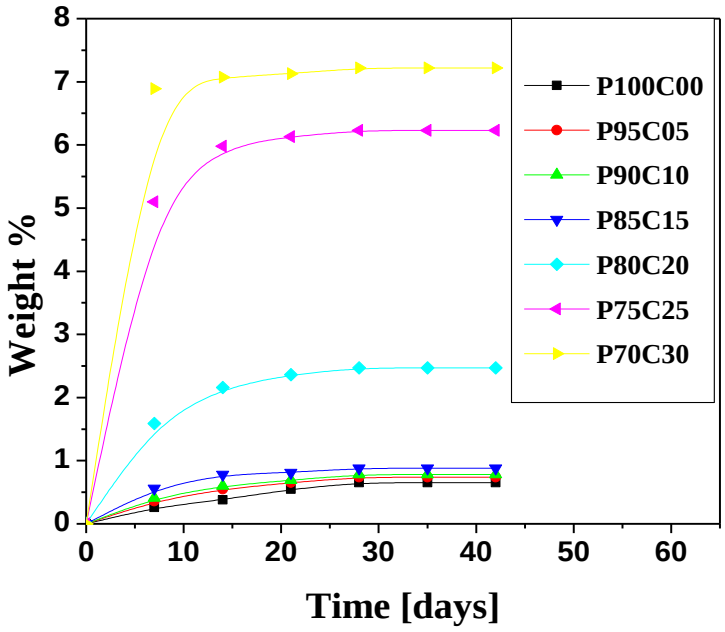

Figure 5.1: Weight % water uptake versus immersion time in days for un-inoculated HDPE/CELL blends.

From the graph, it is evident that there was little water uptake in the pure HDPE (P100:C00). This resistance to the water absorption capacity by the pure HDPE was contributed to by the hydrophobicity of the polymer matrix. The water diffusion was strongly influenced by cellulose content as showed by the higher weight percentage of HDPE/CELL: 70/30. Bio-based synthetic polymers tend to absorb water due the presence of hydroxyl groups in the biopolymers. Starch and cellulose do form hydrogen bonds with water due to their polar character (Bhattacharya and Mani, 1998). Since cellulose is highly hydrophilic, it's a higher affinity for water molecules and thus the high content of cellulose in HDPE influenced higher water uptake. There was a sharp increase of water absorption during the first seven days which then slowed down reaching equilibrium. The progressive decrease in the rate of water uptake with duration of immersion could be due to a concentration gradient across the two materials of the blend. The initial water

molecules added to cellulose particles have been found to be strongly bonded as in a hydrate. This is in consonance with Danjaji *et al*. (2002) who reported that a rapid moisture uptake was observed within the first 14 days of immersion, but this decreased gradually with time.

The blends containing 20 %, 25 % and 30 % of cellulose showed higher water uptake and those blends containing 0 %, 5 %, 10 % and 15 % of cellulose content differ slightly from each other. This was expected due to the low concentration of cellulose particles near the blend surfaces while the rest were positioned deep in the matrix. The interior cellulose particles were not available for hydrogen bonding with the water molecules since they were trapped in the HDPE matrix. Higher cellulose loading made it possible for the cellulose particles to crowd in the blend resulting into its higher concentration near the blend surface. The exposed cellulose particles readily interacted with the water molecules leading to increased moisture uptake.

5.2.2 Effect of inoculation by *Aspergillus niger* on water uptake

Cellulose is a biopolymer that degrades when exposed to the fungi and bacteria environment. HDPE is formed by carbon-carbon (C-C) linkages in which these linkages are not susceptible to microbial attack. The presence of alkyl groups which are non-polar also offer an increased resistance to moisture uptake. Cellulose when blended with HDPE introduces hydroliphic characteristics into the polymer matrix thereby increasing the moisture infiltration tendency as well as microbial attack. HDPE/CELL blends when exposed to a strain of *Aspergillus niger*, the fungus attacks the hydrogen bonds in the

cellulose zones in the matrix which is entirely utilized as the sole provider of energy for the fungus. During inoculation of the diffusion samples, the growth of *Aspergillus niger* colony increased with cellulose loading. This observation is consistent with the results presented by Akaranta and Oku, (1999). They reported that pure polyethylene films showed no evidence of biodegradation and the growth of *Aspergillus niger* increased as the starch loading increased. Inoculation thus creates holes and voids in the HDPE/CELL blends making the polymer perforated. This in turn creates room for water infiltration in the polymer.

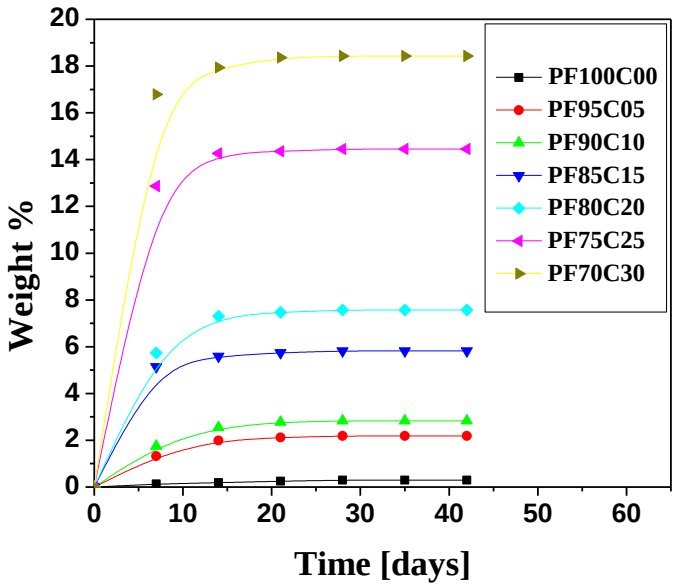

Figure 5.2: Weight % of water uptake compared to the original weight of the specimen against immersion duration in days for inoculated HDPE/CELL blends.

From figure 5.2, it can be deduced that percentage water uptake depends on both cellulose concentration and inoculation. *Aspergillus niger* assimilated the cellulose making the blends perforated and thus enhancing diffusion of water in the HDPE/CELL blends. Compared to the un-inoculated blends, the increase in the moisture uptake is

higher during the initial days of immersion which then consecutively and progressively decreases reaching a plateau on saturation. Therefore, the inoculated HDPE/CEL blends allow a higher moisture uptake than the un-inoculated HDPE/CELL blends and that is probably due the impact caused by the fungus. Figure 5.3 shows a summary of the behavior of diffusant intake before and after inoculation.

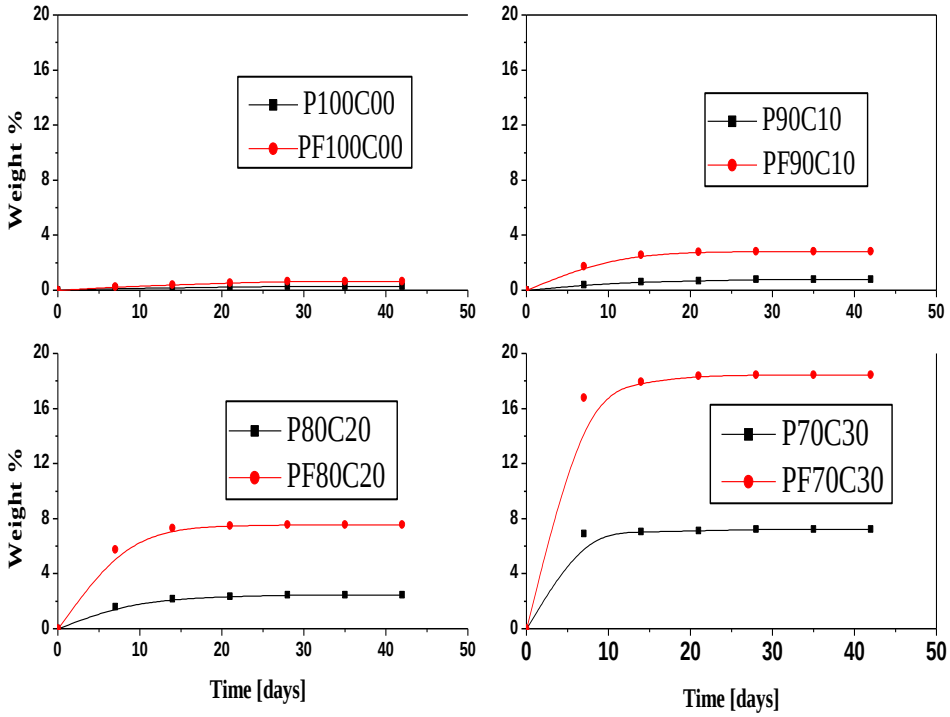

Figure 5.3: Effect of inoculation on weight % of selected HDPE/CELL blends.

5.2.3 Determination of diffusion coefficients

The weight gain resulting from moisture absorption can be expressed in terms of two parameters, the diffusion coefficient or diffusivity, D , and the maximum moisture

content, M_{max} as given by equation 3.40 (Mohd and Berry, 1994). Figure 5.4 displays representative Fickian diffusion plots of M/M_{max} versus $t^{1/2}$ for both un-inoculated and inoculated HDPE/CELL blends in distilled water. The initial linear curve indicates that diffusion followed a Fickian process. Diffusivity is determined from the initial slope of the plot (slope is $D^{\frac{1}{2}}$). The results are summarized in Table 5.1.

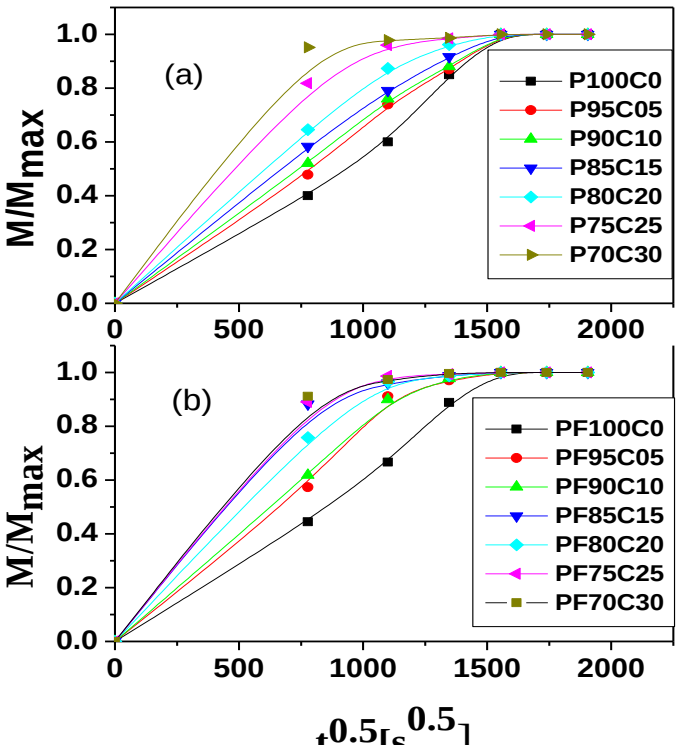

Figure 5.4: Combined Fickian curves HDPE/CELL blends (a) un-inoculated (b) inoculated.

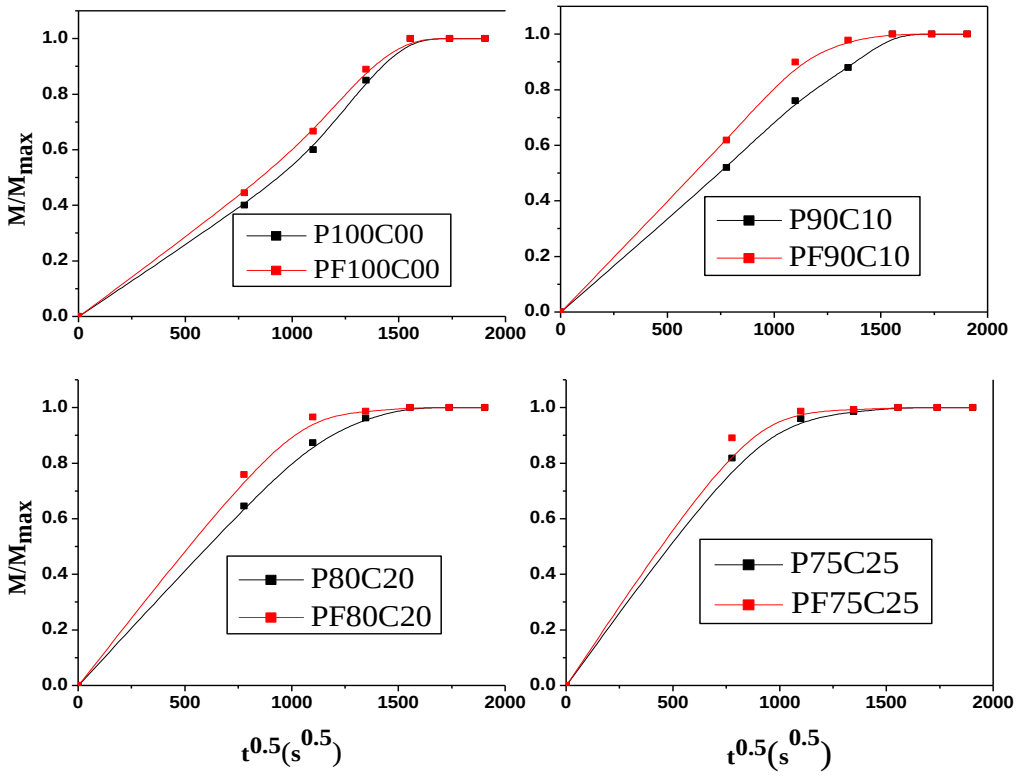

Figure 5.5: Fickian diffusion curves showing comparison between inoculated and un-inoculated.

Diffusion coefficients for the fourteen matrices/blends are given in Table 5.1.

Table 5.1: Fickian diffusion coefficients for un-inoculated and inoculated HDPE/CELL blends.

%HDPE: %cellulose	Diffusivity,$\times 10^{-8}$(cm^2/s)	
	Un-inoculated	Inoculated
100 : 0	0.59±0.40	0.66±0.98
95 : 5	0.76±0.62	1.16±0.43
90 : 10	0.81±0.60	1.19±0.87
85 : 15	0.91±0.38	1.24±0.78
80 : 20	1.25±0.29	2.02±0.69
75 : 25	1.97±0.70	2.44±0.99
70 : 30	4.76±0.57	5.56±0.88

Higher M_{max} and D values are seen in blends having higher concentration of cellulose as well as those blends that have been inoculated. These results can be attributed to the increased hydrophilic nature of the HDPE/CELL by virtue of the presence of an abundance of hydroxyl groups which are available for interaction with the water molecules.

5.2.4 Effect of inoculation on water diffusivity

Inoculation is seen to increase the diffusivity of water in the blends with inoculated ones exhibiting higher D values. This explains the impact of *Aspergillus niger* which created pores, micro-cracks and flaws in the polymer matrix thereby enhancing water uptake. The process is also reinforced as the cellulose loading increases which injects polar functional groups that promotes increased sorption of polar penetrant. Figure 5.6 gives an insight on the effect of cellulose and inoculation on the diffusivity of HDPE/CELL blends.

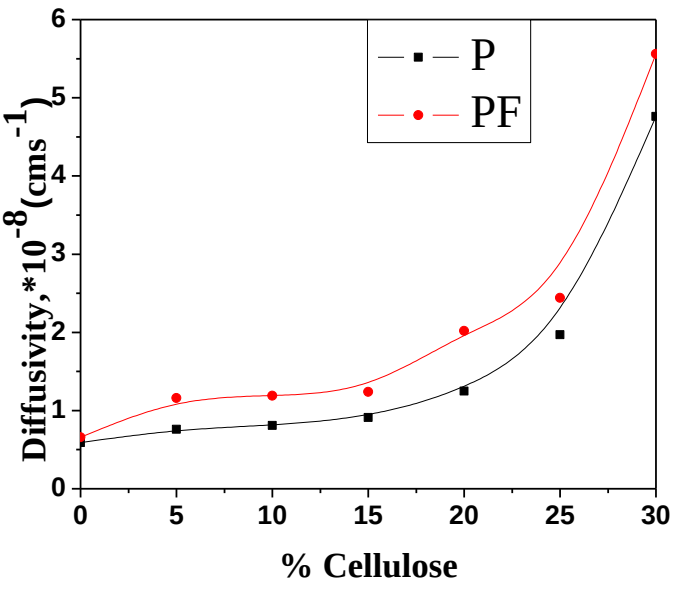

P- Un-inoculated samples

PF- Inoculated samples

Figure 5.6: Effect of cellulose and inoculation on diffusivity of HDPE/CELL blends.

The equilibrium mass intake of each sample is increased with increase in cellulose loading and inoculation. As shown in figure 5.5, an initial linear relationship between M/M_{max} and $t^{1/2}l^{-1}$ is observed followed by a region concave to the abscissa in each case, followed by saturation. Thus this water uptake behavior of HDPE/CELL blends can be characterized as Fickian.

5.3 Thermal-gravimetric analysis results

5.3.1 Thermal stability of the blends

All the HDPE/CELL samples both inoculated and un-inoculated were analyzed to study their thermal stability and to obtain their kinetic parameters which give information about the thermal decomposition process of these blends. The parameters may be used to reveal the changes that occur in the molecular chains as a result of the thermal degradation process. TGA of un-inoculated HDPE/CELL blends are shown in figure 5.7.

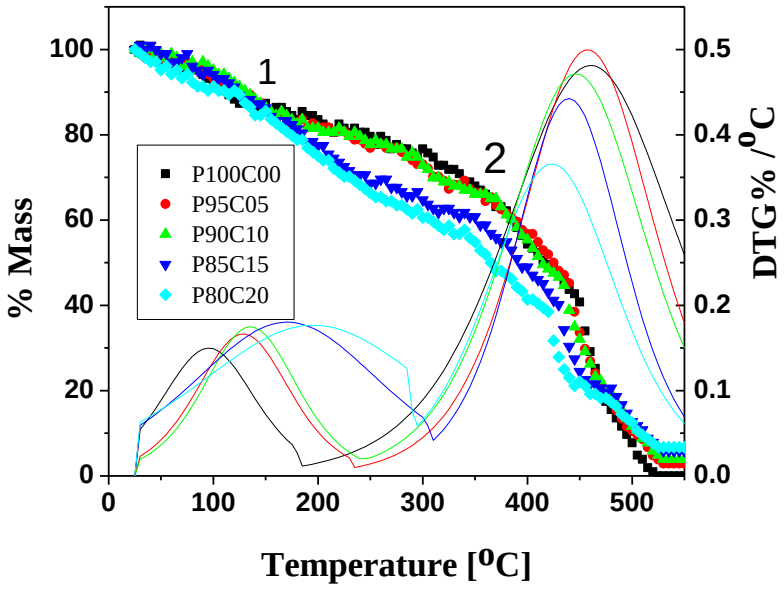

Figure 5.7: TG and DTG curves of HDPE and its CELL blends.

It is apparent from figure 5.7 that weight loss occurred in a two-step process. Specifically, two well-defined stages can be observed in the TG and DTG thermo-grams of all the samples. **Stage 1** is characterized by random chain scission, branching and breakage of glucosidic linkage in cellulose. This is a secondary thermo-degradation process occurring between 50 ^{o}C and 200 ^{o}C during which slight mass loss was registered. This is attributed to the initial moisture trapped in HDPE matrix (Lomakin *et al*., 2011). **Stage 2** is due to pyrolysis of HDPE backbone. This stage represents the main weight loss occurring at a temperature range of (350 ^{o}C-480 ^{o}C) and is assigned to the complete degradation of the carbon chains of the HDPE matrix, which constitute the main component of the samples. For both stages, the rate of mass loss and ash content increases with cellulose loading. The phenomena leading to mass loss due to thermal degradation can be better studied using the derivative mass loss curves which show the rate at which materials decompose (Tajividi and Takemura, 2009).

The highest weight loss occurred at 461.2 ^{o}C for the pure HDPE. This explains the presence of a maximum peak in the derivative weight loss curve (DTG) at 461.2 ^{o}C as shown in figure 5.7. The results also show that the peak decomposition temperatures (T_c) of stage 2 are higher than those of stage 1 since the former stage is assigned to main decomposition of HDPE whose strong covalent bonds require greater heat energy to dissociate. This degradation is due to the fact that HDPE is composed of C-C bonds in the main chain, thereby allowing a temperature increase promotes random chain scission, with associated thermal degradation and de-polymerization occurring at the weak sites of the HDPE main chain (Kim *et al*., 2004). T_c for stage 1 increases with CELL intake due

to increase in the glucosidic linkages in cellulose while T_c for stage 2 decreases with increasing CELL intake due to the decrease of the HDPE backbone. This in turn leads to decreased thermal stability of the blends. Peak thickness for stage 1 increases with cellulose loading with the blend with 20 % cellulose being broader. This effect is as a result of increased fraction of cellulose and its heterogeneity in the matrix. Conversely, the trend in stage 2 is such that peak thickness narrows with cellulose intake due decreased fraction of HDPE in the blend matrix. Above 500 ^{o}C, the quantity of HDPE residue was very small due to its breakdown into gaseous products at higher temperature. The thermal degradation of all the blends was retarded above 500 ^{o}C because of the increased ash content. Table 5.2 gives a summary of the peak decomposition temperatures of HDPE/CELL blends obtained from the DTG curves.

Table 5.2: Peak decomposition temperatures of un-inoculated HDPE/CELL blends.

SAMPLE	T_C (^{O}C)	
	2nd stage	1st stage
P100C0	461.2 ±2.31E-13	93.1±4.43E-14
P95C5	457.4±8.23E-14	133.4±6.23E-13
P90C10	448.4± 7.25E-14	141.5±8.07E-13
P85C15	438.6± 9.19E-14	172.0±7.21E-14
P80C20	424.3± 8.29E-14	200.1±5.37E-14

The peak decomposition temperature for pure un-inoculated HDPE of 461.2 ^{o}C is close to the value of 470 ^{o}C reported by (Fatih and Kadir, 2007). The peak decomposition temperature reduced with cellulose content hence subsequent decrease in thermal stability.

5.3.2 Effect of inoculation on thermal stability of the blends

The HDPE/CELL samples both inoculated and un- inoculated have been analyzed by TGA to establish the effect of *Aspergillus niger* fungus on the thermal degradation and more so the peak decomposition temperature of the blends. The effect of cellulose and inoculation on the peak decomposition temperature is summarized in figure 5.8.

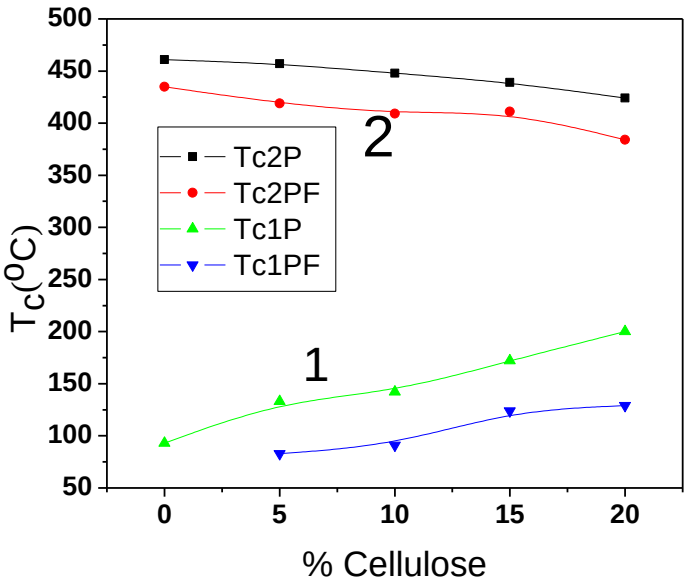

P- Un-inoculated samples

PF- Inoculated samples

Figure 5.8: Effect of inoculation on the T_c of the HDPE/CELL blend.

The effect of inoculation on the peak decomposition temperature for both stages is clearly seen from figures 5.8 whereby the peak decomposition temperature of un-inoculated blends are higher than the inoculated ones due to continuous polymer chains in the un-

inoculated ones. Certainly, inoculation by *Aspergillus niger* perforated the HDPE matrix which required less heat energy to thermo-degrade. This in turn lowered the decomposition temperature. $T_{c\ p100}$= 461.2 ^{o}C, $T_{c\ pf\ 100}$=434.7 ^{o}C, $T_{c\ p80}$=424.3 ^{o}C, $T_{c\ pf80}$= 383.7 ^{o}C. The effect of inoculation improved with increase in the cellulose loading due to the presence of hydroxyl groups in cellulose that provided comfortable zones for attack by *Aspergillus niger*.

5.3.3 Activation energy

The Broido method (Broido, 1969) has been used to evaluate the kinetic analysis of the main thermal decomposition process for both inoculated and un-inoculated blends. Figure 5.9 shows the activation energy plots for the un-inoculated HDPE/CELL blends.

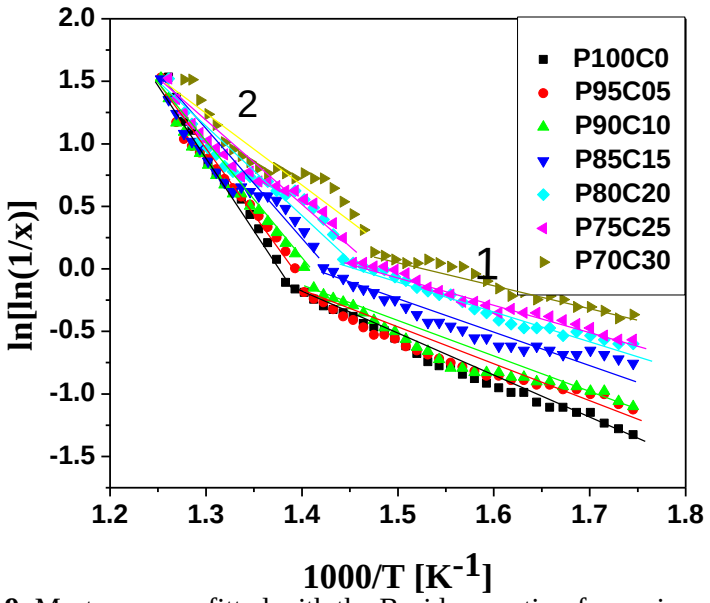

Figure 5.9: Master curves fitted with the Broido equation for un-inoculated HDPE/CELL blends.

The activation energy was determined to describe the energy consumption of the initiation of the thermal degradation process. The analysis of the activation energy of the

blends was carried out based on the Broido equation and adjusting experimental values to the following equation;

$$\ln\ln\left(\frac{1}{x}\right) \cong -\frac{E_a}{RT} + \ln\left(\frac{RZ}{\beta T^2{}_{Max}}\right) \tag{5.2}$$

The graphs in figure 5.9 are linear for both stages hence in total consonance with the Broido equation. The activation energy of each blend was obtained from the slopes of the plots lnln(1/x) versus 1000/T by multiplying the slope of each graph with the gas constant R. The E_a values are shown in Table 5.3.

Table 5.3: Activation energies for HDPE/CELL blends.

SAMPLE	E_a1 (kJ/mol)	E_a2 (kJ/mol
P100C0	27.4±0.38	100.6±0.53
P95C05	20.5±0.46	81.4±0.53
P90C10	22.0±0.82	74.0± 0.77
P85C15	20.8±0.33	57.3±0.75
P80C20	19.9±0.75	49.9±0.57
P75C25	18.3±0.48	49.0±0.66
P70C30	16.6±0.74	45.7±0.82

There is a significant change in activation energy values between the 1st stage and 2nd stage for HDPE/CELL samples. From figure 5.9, it's evident that the activation energy of 1st stage is less than 2nd stage. This is because the former process is assigned to decomposition of cellulose which decomposes at a lower temperature than HDPE. It can be seen from Table 5.3 that the activation energy of neat HDPE is higher than that of the

blends for both stages. The activation energy is also seen to reduce with cellulose content. The blends containing 30 % loading exhibit lower activation energy indicating lesser thermal stability, whereas those with 0 % and 5 % loading show greater activation energy indicating that these samples have higher thermal stability.

5.2.4 Effect of inoculation on the activation energy of HDPE/CELL blends

Figure 5.10 shows the impact of inoculation on activation energy of the HDPE/CELL blends.

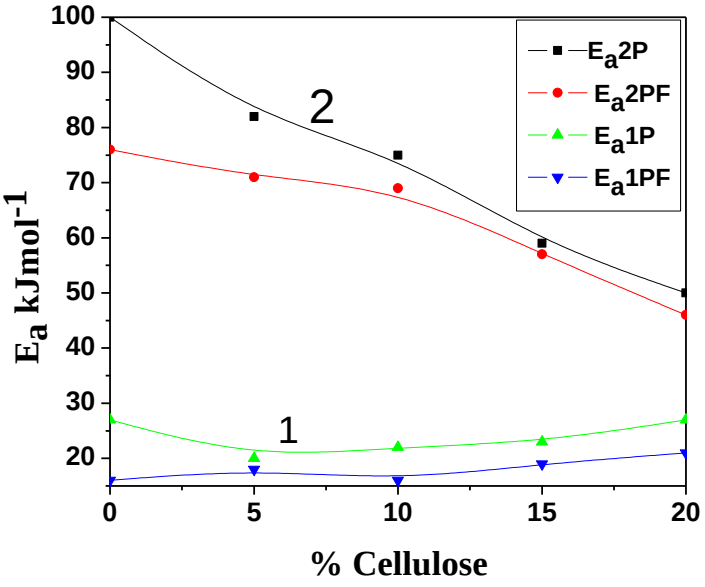

Figure 5.10: Effect of inoculation on the activation energy of HDPE/CELL blends.

Evidently from figure 5.10, activation energy decreases with inoculation since microbial attack causes chain scission, breaking the polymer blends into smaller fragments. The oligomeric chains formed are less temperature resistant. Certainly, when the samples were put in the microbial consortium, the fungus *Aspergillus niger* anaerobically ruptured the chemical morphology of the HDPE matrix thereby lowering the energy required to initiate thermal degradation. The impact of the fungus on the E_a was more felt in blends

with higher cellulose concentration as shown in Table 5.4. This may be due to the fact that cellulose introduced the hydrophilic sites for better attachment of the fungus which in turn bore the holes in the polymer matrix hence weakening the structure. The inconsistency in the E_a values especially for process 1 can be attributed to the method used and experimental errors especially in-homogeneity during mixing of cellulose and the polymer.

Table 5.4: E_a values for HDPE and its blends showing both processes before and after inoculation.

SAMPLE	E_a (kJ/mol)			
	Un-inoculated		Inoculated	
	1^{st}	2^{nd}	1^{st}	2^{nd}
P100 C0	100.6±1.38	27.4±0.54	76.3±2.98	16.4±0.77
P95 C5	81.4 ±1.11	20.5±4.76	72.6±0.75	18.0±1.76
P90C10	74.0 ±4.32	22.0±3.87	69.2±0.75	16.2±0.87
P85 C15	57.3± 3.86	18.6±5.85	65.8±1.18	18.7±2.00
P80C20	49.9±7.03	19.9±2.64	46.3±0.99	21.2±2.51
P75C25	49.0±2.93	18.3±1.98	43.0±2.11	17.8±1.03
P70C30	45.7±3.53	16.6±2.42	42.3±2.34	16.0±0.95

5.4 Creep

Creep is a progressive deformation of a material at constant stress. Creep is a typical characteristic of plastics. It controls the design of many structures and provides motivation for advent of fibre-reinforced polymers. To determine the creep behavior of a material, a constant load is applied to the specimen maintained at a constant temperature and the strain of the specimen is determined as a function of time. It is a combination of behaviors of viscous liquids and elastic solids. Creep in polymers occurs by chains untangling and slipping relative to one another. The extent of deformation under creep depends upon size of the load, time, temperature and the structure and morphology of the polymer (Painter and Coleman, 1994)

5.4.1 Creep strain

5.4.2 Effect of cellulose on the creep strain and recovery

Strain refers to change in length when a material is subjected to high or low temperatures. From the creep data, the percentage creep strain was plotted against time. Figure 5.11 shows creep strain and recovery curves of HDPE/CELL blends at different cellulose loading levels.

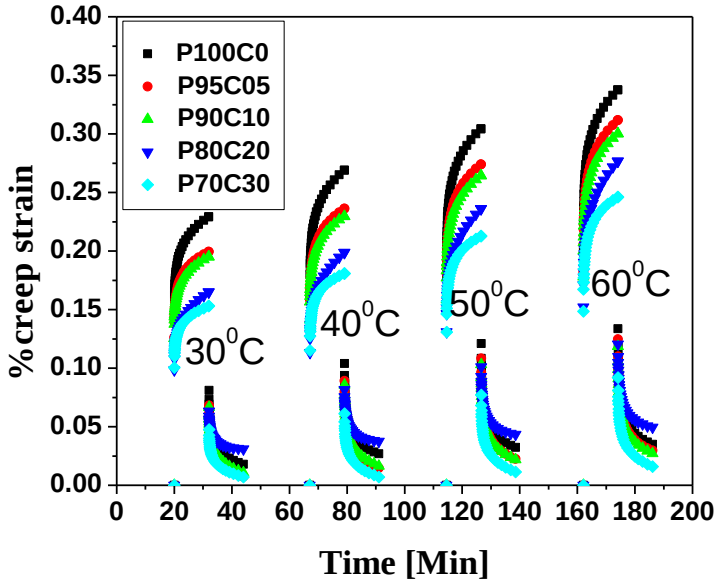

Figure 5.11: Creep strain as a function of HDPE/CELL blends containing 0 %, 5 %, 10 %, 20 % and 30 % at temperatures: 30 ^{o}C, 40 ^{o}C, 50 ^{o}C and 60 ^{o}C.

From figure 5.11, it can be seen that creep strain increases with increase in temperature. This is attributed to the softening of the molecular chains of the polymer as temperature rises. Further still, the curves shows that creep resistance increases with cellulose loading (Mancia, 1974). As the cellulose content increases, the deformation decreases as should be expected from increased rigidity of the blends. There are clear trends that increase in cellulose percentage led to better resistance of the blends with the blend having 30 % cellulose registering the highest creep resistance. These results indicate that cellulose played two important roles on the creep mechanics of the blends:

Free volume effect: Introducing cellulose in the HDPE matrix largely reduced the relative volume of viscoelastic polymer matrix leaving less material to creep under stress and improving the overall creep resistance.

Bridging effect: The cellulose particles sustained part of the stress by forming an interconnected network which in turn lowered the creep strain.

Recovery is the ability of a material to return to its original state once the stress or stretching force acting on it has been removed. The recovery dynamics of the blends was more complicated with the blend having 20 % cellulose recovering less compared to pure HDPE. The recoverability of the blends didn't show a clear trend with different loading levels of cellulose. However, it can be deduced that cellulose improved the recoverability of the blends due of attraction OH groups hence good creep performance. On the overall, addition of cellulose improved the creep property of HDPE by increasing both instantaneous modulus and long term viscosity. The percentage cellulose loading level of 20 % resulted in the best effect based on the two parameters.

5.4.3 Effect of inoculation on creep strain and creep recovery

From creep data of both un-inoculated and inoculated HDPE/CELL blends, the percentage creep strain was plotted against cellulose as shown in figure 5.12.

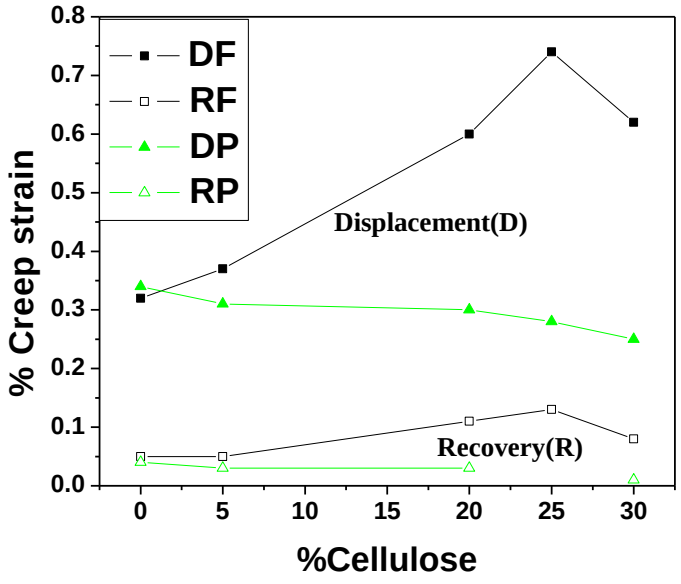

F- Inoculated samples

P-Un-inoculated samples

D-Displacement

R-Recovery

Figure 5.12: % creep strain and recovery as a function of CELL of HDPE/CELL.

It can be inferred from the curves that creep resistance decreases with inoculation as cellulose increases during displacement. The polarity of cellulose makes its dispersion in the HDPE matrix poorer and the tendency towards flocculation and aggregation is expected. The agglomerates are easily broken during an impact test and contribute to decreased creep resistance of the blends (Kim *et al*., 1998). The fungi species *A.niger*, attacked the agglomerates using them as sole carbon source rupturing the blends by creating holes and voids. This led to poor adhesion between cellulose and the polymer matrix hence little effect in stabilizing the HDPE molecular chains. The exposed neighboring C-C bonds constrained the matrix flow significantly resulting in a deteriorating matrix embrittlement. The effect of *A. niger* was more pronounced at higher cellulose levels whereby the probability of particle agglomeration increased and created regions of stress concentration that required less energy to initiate or propagate a crack hence reduced creep resistance with inoculation. The recoverability of the blends decreased with inoculation because of the destroyed molecular chains leading to less stress transfer from chain to chain.

5.4.4 Creep compliance

The creep compliance behavior of HDPE/CELL blends as a function of time at different testing temperatures is shown in figure 5.13. It is evident from the curves that creep compliance increases with temperature due to increasing polymer chain mobility.

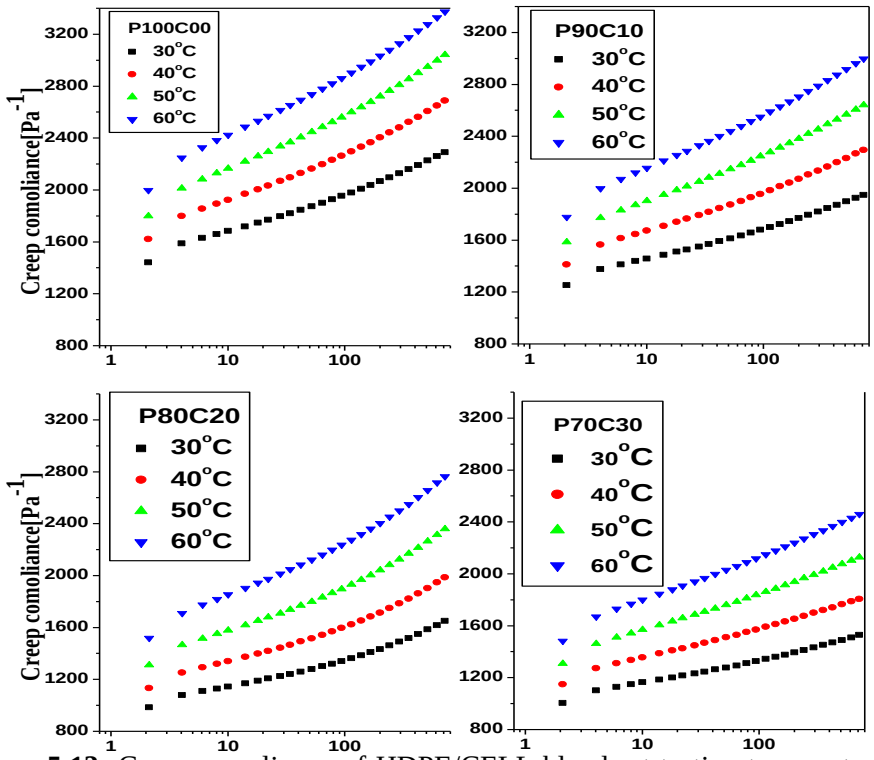

Figure 5.13: Creep compliance of HDPE/CELL blends at testing temperatures 30 °C, 40 °C, 50 °C, and 60 °C.

5.4.5 Effect of cellulose on creep compliance

Creep compliance is greatly influenced by adhesion and consolidation (Izer *et al.*, 2009). It is clear from the curves of figure 5.13 that creep compliance decreases with cellulose content with the blend containing 30 % cellulose registering lower values of creep compliance compared to neat HDPE. Creep compliance reduces with consolidation of the particles. Introducing cellulose to the HDPE matrix increased its density (better consolidation, low void content) and creep compliance decreased as expected.

5.4.6 Effect of inoculation on creep compliance

Figure 5.14 shows comparison curves obtained from un-inoculated and inoculated data of HDPE/CELL blends at a temperature of 30 °C.

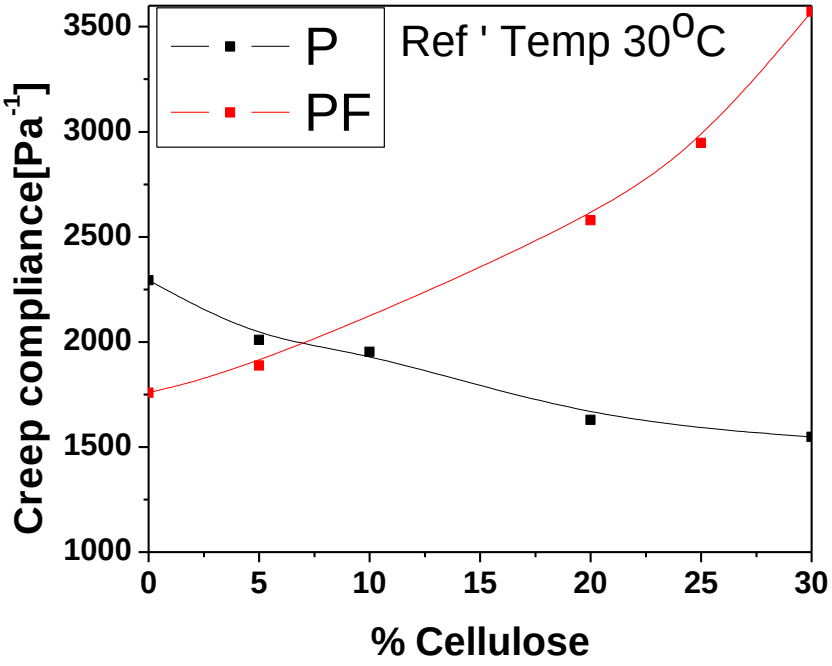

Figure 5.14: Effect of *Aspergillus niger* on creep compliance of HDPE/CELL blends at testing temperature 30 °C.

The curves show opposite trends, whereby the creep compliance of un-inoculated blends decreases while that of inoculated ones increases. This is due to the effect of *A.niger* which ruptured the polymer matrix hence increasing the overall chain motion. The effect of inoculation was more prominent in the blend with higher cellulose content (30 %) which had the highest values of creep compliance. Increased cellulose levels significantly reduced the polymer part in the blend and because of its polarity; there was poor adhesion between the polymer and cellulose leading to improved creep compliance. Besides, *A.niger* has a high affinity for cellulose because of the presence of hydroxyl groups and thus its high content provided comfortable regions for its attachment utilizing it as food. This in turn increased the void content and density reduced (poor consolidation) and an increase in creep compliance.

5.4.7 Time –temperature superposition (T.T.S)

One of the most useful extrapolation techniques for creep is T.T.S. The technique can be used to predict long term creep behavior of polymers by shifting the curves from tests at different temperature horizontally along the logarithmic time axis to generate a single master curve at low temperature (Tajividi and Tekemura, 2009). By selecting the reference curve as 30 ^{o}C, and then shifting all other isothermal curves of the creep compliance against time obtained at 30 ^{o}C, 40 ^{o}C, 50 ^{o}C and 60 ^{o}C with respect to time horizontally, the master curves of creep compliance with time were obtained as shown in figure 5.15.

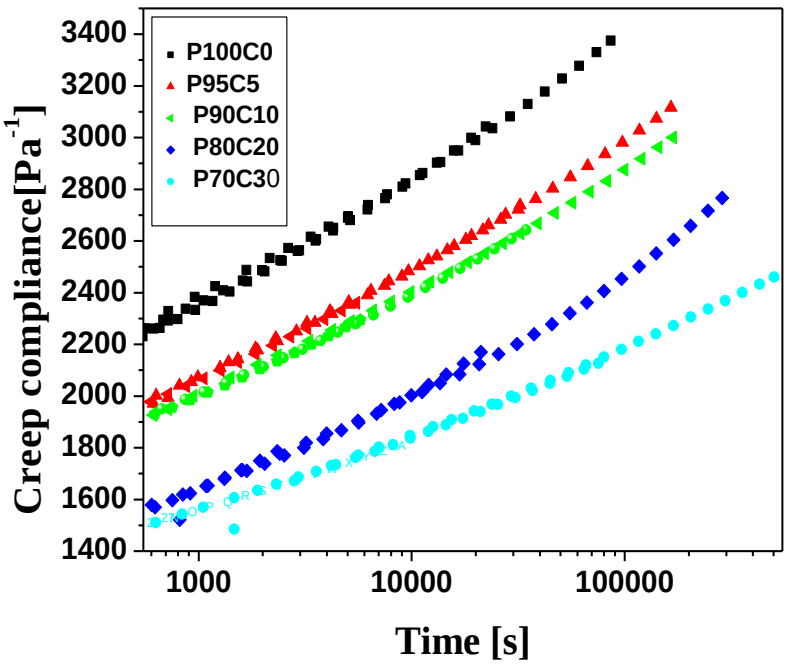

Figure 5.15: Creep compliance master curves from shift data for HDPE/CELL blends.

The creep master curves shown in figure 5.15 were obtained by shifting creep curves at different temperatures with reference temperature chosen at 30 ^{o}C. A relatively good

agreement can be observed but the curves tend to deviate from each other at longer times. Such a trend was reported by (Marias and Villoutrex, 1998). This indicates that the effect of temperature on the creep behavior is much more pronounced than the effect of time. This can be clearly seen as the master curve deviates from actual creep curve at longer times (higher temperatures). From the curves it can be deduced that at short time intervals the blends exhibited high creep compliance while at longer time's viscous flow occurred and the blends exhibited relatively high creep compliance. At shorter time intervals, because of the polarity of cellulose, there would be poor adhesion and reduced consolidation leading to increased creep compliance in the HDPE matrix. Creep compliance is very high for HDPE/CELL blends at short times because of increased re-orientation and motion of the polymer chains in the HDPE. As time increases the creep compliance decreases this is due to the fact that stress relaxation rate decreases as free volume diffuses out making the blends stiffer and brittle. From figure 5.15, one would be able to predict the creep behavior of HDPE/CELL blends for a time of 5×10^6s i.e 58 days from an experimental time span of 12 minutes. The T.T.S fits obtained from the WLF equation by shifting the logarithmic time axis are shown in figure 5.16.

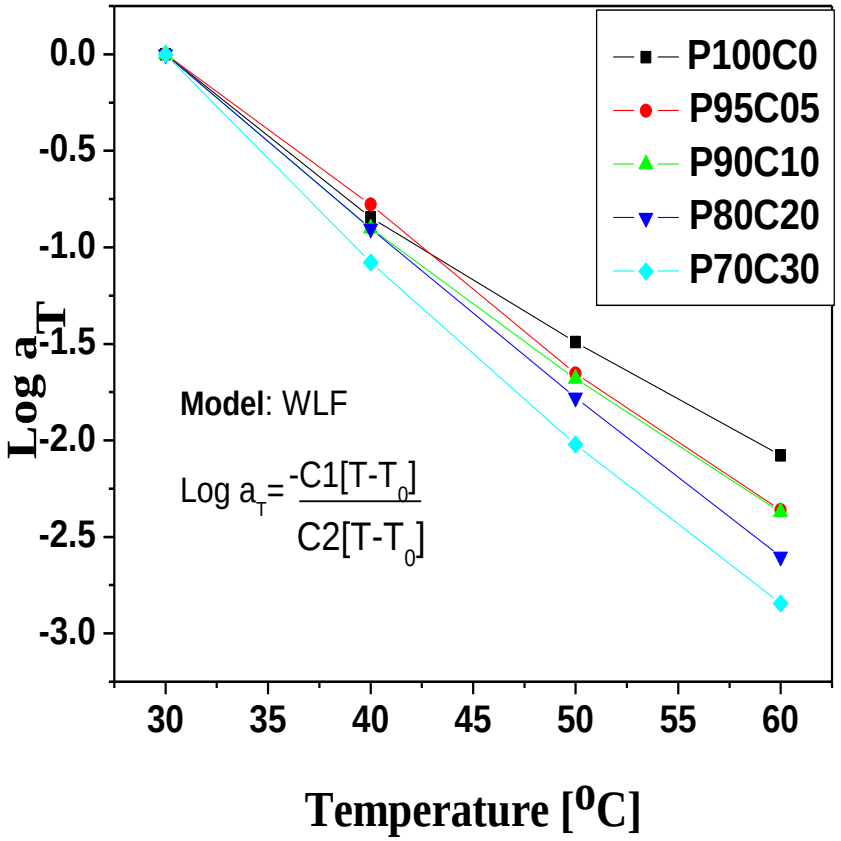

Figure 5.16: Temperature dependence of the shift factor a_T for HDPE/CELL blends.

The shift factor is a measure of how a material's frequency response changes with the variation of temperatures. Experimental data for shift factors was tested with WLF model. The curves are in good agreement with the WLF equation indicating that the deformation depends on free volume. The shift factors are seen to decrease with cellulose percentage due to decreased deformation. The values of C1 and C2 obtained from the WLF equation are shown in Table 5.5.

Table 5.5: WLF fit parameters.

Cellulose %	C1	C2	T_o (^oC)
0	8.3±0.42	90.0±5.76	30.1±0.30
5	9.1±0.50	132.9±3.56	30.0±0.10
10	12.9±1.40	134.0±24.11	30.0±0.25
20	13.2±2.90	142.6±16.01	30.1±0.10
30	15.6±2.33	198.4±21.21	30.0±0.30

From Table 5.5 it's evident that the values of C1 and C2 increased with cellulose loading. These values usually depend on the sample morphology and thus their increase suggests a change in free volume as temperature increases (Champion *et al*., 2001).

5.5 Dynamic mechanical analysis

DMA test methods have been widely used for investigating viscoelastic behavior of composite materials. The storage modulus E', determines the ability of the material to absorb or store energy; higher E' indicates more rigid material. The loss modulus E'' determines the ability of the material to dissipate energy. A high E'' indicates good damping properties (Khalid *et al*., 2009).

5.5.1 Effect of frequency on viscoelastic behavior in HDPE

The viscoelastic properties of a material are dependent on temperature and time (frequency). If a material is subjected to a constant stress its elastic modulus will decrease over a period of time. This is due to the fact that the material undergoes molecular

rearrangement in an attempt to minimize the localized stresses. The phase-transition in the HDPE was investigated using DMA during heating the sample from -30 ^{o}C to 120 ^{o}C at seven frequencies 1, 3, 5, 10, 15, 20 and 30 Hz. The spectra are shown figure 5.17. The fits in figure 5.17 (b) were obtained from loss fit equation below.

$$E^{"}(T) = \sum_{i=1}^{2} A_i \exp\left\{-\frac{E_i}{kT} - \frac{T^2}{T_{m_i}^2}\exp\left[\frac{E_i}{k}\left(\frac{1}{T_{m_i}} - \frac{1}{T}\right)\right]\right\} \tag{5.3}$$

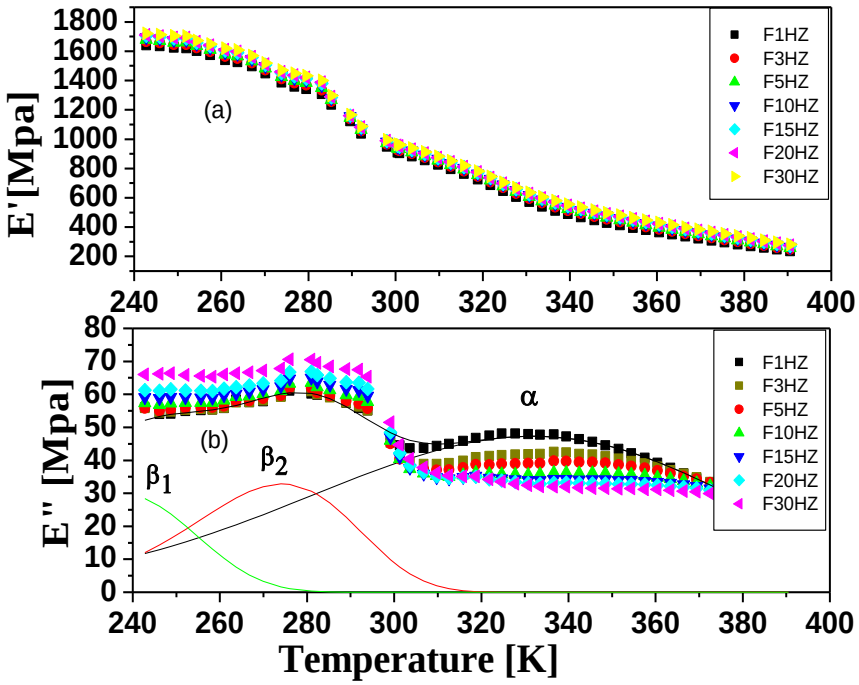

Figure 5.17: a) E' as a function of temperature (b) E'' as a function of temperature showing relaxation spectra at different frequencies for P100C00.

From figure 5.17 (a), it's evident that storage modulus increases with frequency. This is attributed to the lesser mobility of polymeric chains at higher frequency. Modulus measurements performed over a short time (high frequency) result in higher values whereas measurements taken over long times (low frequency) result in lower values. Three transitions can be seen from the E'' spectra (figure 5.17-b). The α transition which is related to the main chain motion (T_g). β is related to inter-lamellar shearing. The

Presence of β_1 and β_2 indicates two lamellar types. The α-process shifts to higher temperature with increasing frequency and is the true relaxation while β-process is frequency independent as result of inherent structural stress. The α peak decreases in intensity as the frequency increase, but shift to higher temperatures. In addition, the maximum of the peak decrease with increasing the frequency. That is the loss modulus decreases with increasing the frequency, which, indicate a relaxation process.

This decrease in the intensity of the loss modulus peak as frequency is increased can be attributed to the fact that at high frequencies the chains are not allowed enough time to respond to the applied sinusoidal strain and it becomes quite difficult for the chains to follow the movement of the oscillation. Only a few, probably those with shorter chain lengths are able to oscillate giving a lower value of loss modulus. In the case of low frequency, chains are given time to respond to the applied strain and almost all the chains are able to follow the movement of the oscillations, resulting in a high value of loss modulus. As the temperature increases the polymer softens allowing more chains to take part in the oscillations and hence an increase in the loss modulus as initially observed. However, HDPE being a highly crystalline material crystallizes when the temperature is raised above the glass transition temperature, T_g. Temperature increase enables substantial parts of the chain to extricate themselves from their entanglements and align in a more cohesive crystalline manner (Billmer, 1984; Hay, 1995; Stevens, 1990). This formation of crystallites affects the segmental mobility due to restrictions and limitations imposed by crystallites and trapped entanglements, as a result the number of chains participating in the relaxation process reduces thus reducing the loss modulus. It is

therefore evident that, temperature increase makes the relaxation process faster due to softening of the polymer. However, decrease in intensity is due to chain constraints imposed by crystallization.

5.5.2 Relaxation spectra for storage modulus and loss modulus

Figure 5.18 shows relaxation spectra of storage modulus (E') and loss modulus (E'') at 1 Hz.

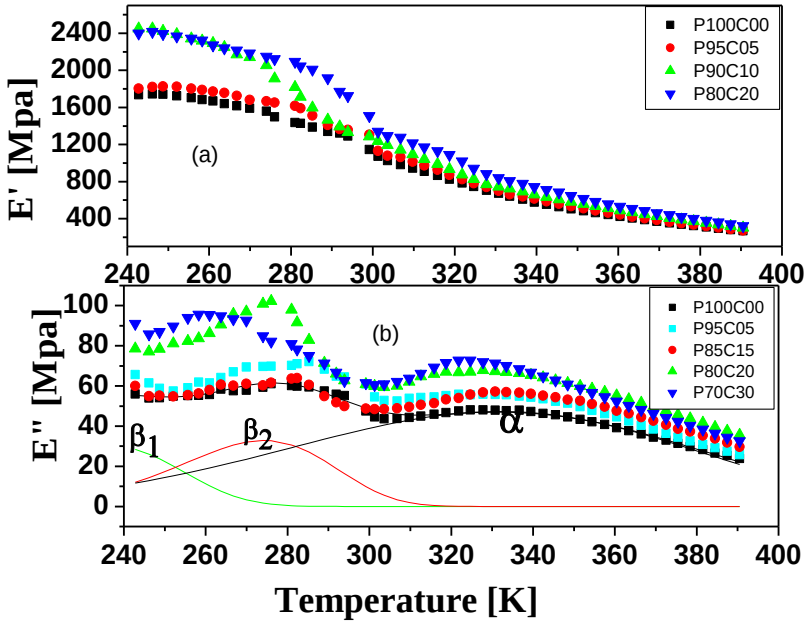

Figure 5.18: (a) Storage modulus (E') and (b) loss modulus (E'') as a function of temperature for HDPE and its CELL blends.

The storage modulus is noted to decrease accordingly with temperature [figure 5.18(a)].

The shape of E' curves (i.e drop, rise, and finally drop) is associated with the crystallization process. The increase in the chain mobility above Tg (153 K for HDPE) favors activation of the crystallization process which proceeds as the temperature increases. This phase transformation continues until the enhanced crystallinity reduces the molecular chains' mobility and crystallization rate of the polymer blends. Generally,

all the blends registered low modulus with increasing temperature due to the softening of the polymer blends. The effect of cellulose is evident from the curves. With increasing cellulose, E' increases indicating that stress was transferred from the HDPE matrix resin to cellulose fiber. The high modulus might be because of two reasons: intra-molecular bonds and rigid skeletal conformation of cellulose fiber (Rodrig *et al*., 1975). This means that the blends with higher percentage cellulose have enhanced stiffness and therefore stores more energy on impact.

E'' spectra for HDPE/CELL blends from -30 ^{o}C to 120 ^{o}C is shown in figure 5.18 (b). For pure HDPE the loss modulus peak (α) is observed around 330 K while the β-peak is at 280 K. The dominant β-peak is due to the glass-rubbery transition of amorphous portions while the shallow α-relaxation shoulder is attributed to main chain motion in the crystalline phase. The loss modulus of the blends was estimated a little higher than the base polymer due to increased molecular environment (OH groups) participating in the process. In short, all the blends registered low modulus with temperature. T_{α} does not change with CELL intake indicating that CELL does not change the free volume of HDPE while T_{β} remains unchanged due to inherent lamella stresses. The intensities of both α and β- relaxation increase significantly with increasing cellulose. The β- transition is related to the glass- rubbery transition which is due to lamella slip associated with the unrestricted amorphous HDPE. α – relaxation shifted to higher temperatures as cellulose loading increased. This can be seen between 310 K and 350 K. The restricted molecular mobility due to interactions between HDPE and cellulose surface contributed to the shift to higher melting temperature T_m. The presence of crystals is necessary for this transition

to occur (Wunderlich and Seyler, 1994). The maximum E'' and the temperature of the maximum loss T_m have been obtained for each relaxation fitting its data using VFT model equation from which the activation curves in figure 5.19 were obtained.

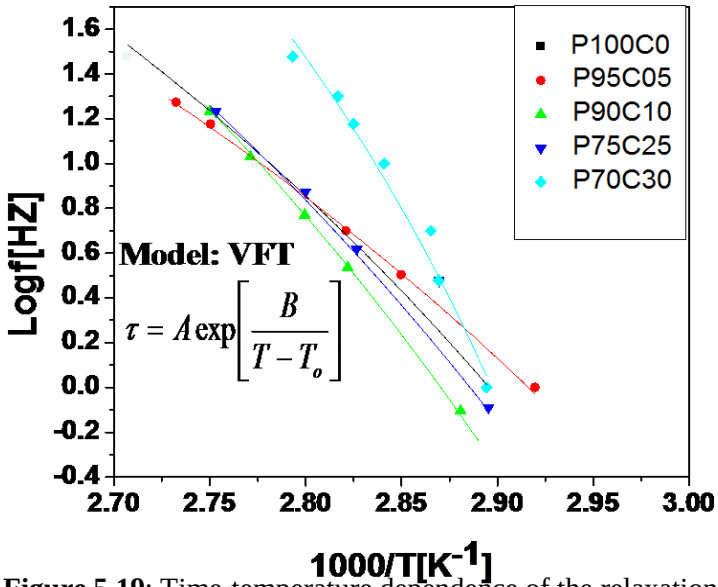

Figure 5.19: Time-temperature dependence of the relaxation process for HDPE/CELL blends.

Table 5.6: The relaxation (VFT) fit parameters for the different relaxation processes in the HDPE/CELL blends.

SAMPLE	VFT parameters		
	A	B	T_o (K)
P100C0	6.4±0.50	485.9±61.56	269.2± 5.20
P95C05	6.4 ±0.60	521.4± 53.20	256.3±1.98
P90C10	7.5±0.73	574.0±23.11	271.6±3.32
P80C20	7.4±0.43	620.0±32.65	263.0±2.86
P75C25	8.7±0.24	616.4±42.10	273.2±3.11
P70C30	8.8±0.50	621.2±25.32	274.6±2.34

The glass transition temperatures for the blends can be obtained by adding 50 ^oC to T_o.

The time-temperature dependence of the mean relaxation frequency (τ) for the blends is shown in figure 5.19. The processes are characterized by the Vogel-Fulcher-Tamman scaling behavior typically to glass transition process. The corresponding VFT fitting parameters are given in Table 5.6. The VFT parameters have been obtained using Vogel-Fulcher-Tamman law (Vogel *et al.*, 1921). From figure 5.19 it can be inferred that α-relaxation which is the main chain motion obeys VFT law. Relaxation frequency shows no trend with CELL intake indicating that free volume is unaffected by its presence.

5.5.3 Effect of inoculation on loss modulus

The effect of *A.niger* on the relaxation zones has been studied in order to analyze in more detail the mechanical behavior of the samples. Figure 5.20 shows the effect of *A.niger* on the intensity of α and β-peaks.

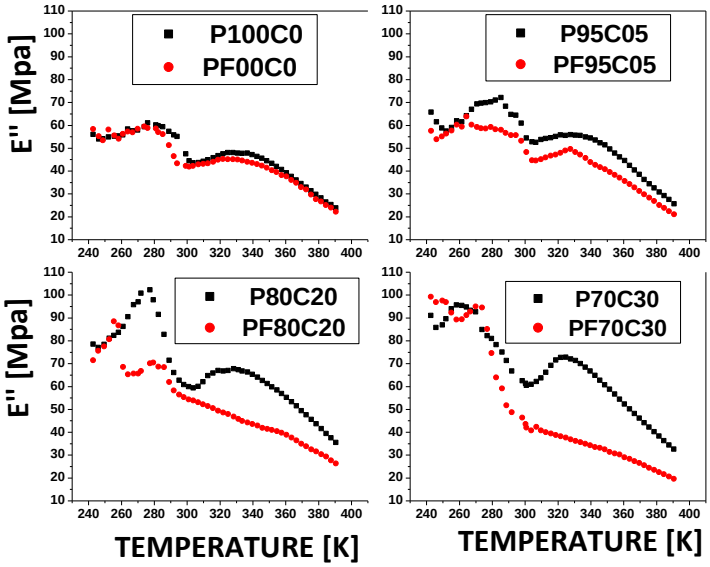

Figure 5.20: Effect of inoculation on the E'' of selected HDPE/CELL blends.

It can be seen from figure 5.20 that inoculation lowers the loss modulus. Intensity of E" decreases on inoculation due to removal of cellulose and formation of oligomers which reduces the stiffness. The α-peak flattens with increased cellulose content in the blends. Long chains perform co-operative motion with little distribution of relaxation times and hence the narrow peak before inoculation. Microbial activities by *A.niger* fragment the long HDPE/CELL chains. Short chains perform segmental motions with wide distribution of relaxation times leading to peak broadening after inoculation. This fact reveals that a transformation in the lamella sizes distribution occurs due to degradation of the blends. This means that the crystalline phase is considerably affected by the degradation of the bends with *A.niger* which tore the polymer matrix forming smaller crystallites. Thinner crystallites are more prone to degradation when attacked by micro-organisms (Ribbes-Greus and Diaz-Calleja, 1987) hence lower E''. An irregular decrease in intensity of the β peak is also noted revealing a certain re-organization of the molecular chains of the crystalline-amorphous interface which were initiated by the fungus so that their motions were less hindered.

5.5.4 Effect of inoculation on storage modulus

Figure 5.21 shows the effect of *A.niger* on the storage modulus of HDPE/CELL blends obtained from DMA data at 1 Hz.

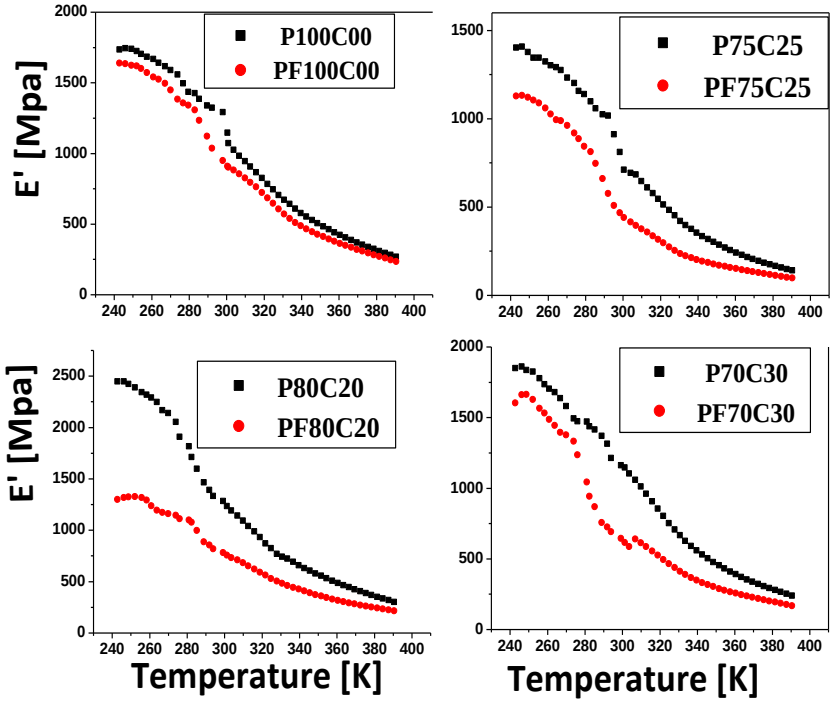

Figure 5.21: Effect of inoculation on HDPE and its CELL blends on storage modulus.

From figure 5.21 it can be observed that the storage moduli of the blends are higher than the neat HDPE. The E' of the inoculated blends are generally lower than the E' for the un-inoculated blends with the trend changing with % cellulose. Intensity of E' decreases on inoculation as cellulose intake increases since the fungus attacks CELL matrix leaving a less stiff HDPE matrix. From these results, it can be argued that *A.niger* utilizes cellulose primarily as its carbon source creating perforations in the blend matrix. This in turn lowers the inter-phase area which significantly reduces the energy stored by the blend.

CHAPTER SIX

CONCLUSIONS AND RECOMMENDATIONS

6.1 Conclusions

Based on this study, there is an effective conclusion that CELL and *A. niger* strongly affected the diffusion, thermal and mechanical properties of HDPE and its blends. Addition of CELL to HDPE accelerated microbial activities by *A. niger* which greatly influenced the fore-mentioned properties. Cellulose has an aggressive behavior of water absorption due to existence of hydroxyl groups that are very attractive to form hydrogen bonding with water molecules. The effect of CELL and *A.niger* on diffusivity of water has been studied following immersion of HDPE and its blends at room temperature. The results show that moisture uptake increases with cellulose content and inoculation. Moisture absorption of pure HDPE was almost 0 %, whereas for HDPE/CELL blends, their moisture uptake increased as cellulose content increased. This ensures that the presence of CELL in the HDPE matrix creates a polar environment which enhances hydrogen bonding. Inoculation by *A.niger* creates micro-cracks, gaps and flaws in the polymer matrix which are key zones for water infiltration. It's important to note that microbial activities increased with cellulose loading since CELL provided comfortable zones for attachment of *A.niger*.

Thermal degradation of HDPE and its blends has been investigated. The TGA and DTG curves showed a two-step thermo-degradation process for all the samples. The main stage has been attributed to the complete decomposition of the carbon backbones of HDPE.

The secondary stage which takes place at temperatures below 200 ^{o}C has been assigned to the thermal degradation of the corresponding cellulose in the blends. In general, the TGA and DTG results have proved that CELL significantly lowers the thermal stability of HDPE as seen from the decreasing thermal decomposition temperatures with CELL loading. Inoculated blends registered faster mass loss and low decomposition temperatures compared to un-inoculated ones. This is attributed to the effect of *A. niger* which assimilated the CELL particles in the blends leaving a perforated HDPE matrix with weak bonds of polymer chains. Thus higher molar mass of HDPE is lowered subsequently leaving less material available to thermo-degrade. The activation energy greatly reduced with cellulose as seen from the Broido fits due to reduced thermal stability. Inoculated blends had the least activation energies since *A.niger* fragmented the polymer backbone forming short chain oligomers which are less temperature resistant.

Cellulose imparts an adverse effect upon the mechanical properties of HDPE and its blends. Storage modulus is increased due to the hydrophilic nature of CELL that is not compatible to the hydrophobic nature of HDPE resulting in weak interfacial adhesion. As CELL loading increases, their cohesive strength becomes stronger than particle-matrix interactions causing high modulus. At any particular temperature, the storage modulus increases with CELL and decreases with temperature. Storage modulus decreases with temperature due to increased viscosity and polymer chain mobility and increases with CELL due the reinforcing action of CELL which improves the matrix stiffness. Loss modulus spectra show three processes. The beta process (β1 and β2) is related to the glass transition of loose ties and loop molecules in the amorphous layers. The alpha (α)

relaxation process is related to relaxation of restricted HDPE amorphous chain in the crystalline phase. Understanding loss modulus spectra is important as it gives information on the overall flexibility and interactions between composite components. Comparing the spectra of un-inoculated and the inoculated blends of a particular composition has shown similar trends and inoculation is seen to lower both the storage and loss modulus of the blends. The peaks intensity decrease with inoculation, revealing that a transformation in the lamellar sizes distribution occurs due to the degradation process. From these arguments, it can be concluded that degradation process by *A.niger* affects just to a small extent the amorphous phase of the polymers.

Creep compliance and creep strain of HDPE/CELL is seen to increase on inoculation. This effect further reinforces the impact of *A.niger* on viscoelastic properties which ruptures the blends by removing CELL particles hence increased deformation. Shift factors obtained from frequency isotherm superposition were applied to creep compliance isotherms at the same temperature and a single horizontal shift factor was not adequate to explain the temperature-dependence of this parameter. The T. T. S curves deviated from each other at longer times (higher temperatures). This indicates that the effect of temperature on the viscoelastic response of such materials is much more significant than the effect of time. Smooth master curves were produced by T. T. S technique through horizontal shifts, but it slightly over-predicted the long term creep for the blends.

6.2 Recommendations

In the natural environment, different kinds of micro-organisms play an important role in various steps involved in the degradation of synthetic polymers in general and their blends in particular. Studying the synergism between these micro-organisms will give an insight for future efforts towards the biodegradation of these materials. Screening or isolating micro-organisms from polymer dumpsite or petroleum waste could lead to new unexplored strains with superior performance. Employing other supplementary measurement techniques like SEM, FTIR would give an insight on the morphology of the blends especially after microbial activities. The superposition of creep curves is not satisfactory, and this indicates that only horizontal shifting is not adequate. Probably, a better superposition can be obtained by application of frequency horizontal and vertical shifts to creep data. This indicates that a two-dimensional superposition method is preferable. The base polymer (HDPE) in this case is thermo-rheologically complex and the presence of CELL adds to its complexity. T.T.S does not work well for such materials and their composites. The use of power law model, would better predict long term creep behavior of such composites. Manufacturing packaging products from plastic/cellulose blend should be adopted as this would improve their hydrophilicity and subsequent biodegradation. Besides, inoculating plastic garbage with *Aspergillus niger* as preliminary step before disposal would largely help in reducing the plastic waste menace.

REFERENCES

Akaranta, O. and Oku, G.I. (1999). Some properties of cassava mesocarp carbohydrate-LDPE blends. *Carbohydrate polymers*, **34**: 403-405.

Albertsson, A.C., Erlandsson, B., Hakkarainen, M. and Karlsson, S. (1998). Molecular weight changes and polymeric matrix changes correlated with the formation of degradation products in biodegraded polyethylene. *Journal of environmental polymer degradation*, **6**: 187-95.

Anthony, G. (1999). Kinetic and chemical studies polymer cross-linking using thermal gravimetry and hyphenated methods. Degradation of PVC. *Polymer degradation stability*, **64**: 353-357.

Australian Marine Conservation Society, (2011). htt://www.amcs.org.au.

Behjat, T., Russly, A.R., Luqman, C.A., Yus, A.Y and Nor Azowa, I. (2009). Effects of PEG on the biodegradability studies of Kenaf cellulose-polyethylene composites. *Journal of international food research*, **16**: 243-247.

Billmer, W.F Jr. (1984). Textbook of polymer science, 3rd Edition. Applied science publishers, Londan: pp 366-367.

Brauman, S.K. (1988). Polymer degradation during combustion. *Journal of polymer science*, **26**: 1159-1171.

Broido, A. (1969). A simple sensitive graphical method of treating thermo-gravimetric analysis data. *Journal of polymer science*, **7**(10): 1771-1773.

Brunella V. and Trossarelli, L. (2003). Polyethylene discovery and growth. University of Torino, Italy.

Chainey, M. (1989). Handbook of polymer science and technology: composites and speciality applications. Mercel Dekker, Newyork, 4: 499.

Champion, L., Gerald, J.F., Planche, J.P., Martin, D. and Anderson, D. (2001). Low temperature fracture properties of polymer modified asphalts relationships with the morphology, Kluver Academic Publishers. *Journal of material science*, **36**: 451-460.

Chiellini, E., Solaro, R., Corti, A., Picci G., Leporini, C., Pera, A., Valini, G. and Donaggio, P., (1999). Degradation of starch-filled polyethylene films in a compositing environment. *Chim Industries*, **8-9**:656-63.

Crank, J. (1975). The mathematics of diffusion, 2nd Edition. Clarendon press, Oxford University, Newyork: pp 100-165.

Danjaji, I.D., Nawang, R., Ishiciku, U.S., Mohd Z.A. (2002). Mechanical properties of sago starch filled LLDPE composites. *Polymer testing*, **20**:167-172.

Doolittle, A. K. and Doolittle, D. B. (1957. Viscoelatic properties of polymeric materials. *Journal of applied physics*, **28**:901.

Fatih, M. and Kadir K. (2007*).* Thermal degradation, mechanical properties and morphology of wheat straw flour filled recycled thermoplastic composites. *Polymer degradation and stability*, **3**:237.

Findley, W.N., Lai, J.S. and Onaran, K. (2007). Creep and relaxation of non-linear viscoelastic materials With an introduction of linear viscoelasticity. Dover publications, Newyork.

Fried, J. R. (1995). Glass transition temperature in polymers. *Polymer science and technology*, **4**: 257.

Gilmore, D.F., Antoun, S., Lenz, R.W., Fuller, R.C. (1993). Degradation of poly(β-hydroxyalkanoates) and polyolefin blends in municipal waste water treatment facility. *Journal polymer environment*, **1**(4): 269-274.

Griffin, G. J. (1994). Synthetic polymers and living environment. *Pure and applied chemistry*, **52**:399-407.

Grija, B.G., Sailaja, R.N. and Giridhar, M. (2005). Thermal degradation and mechanical properties of PET blends. *Journal of Polymer degradation and stability*, **90**: 130-160.

Hadad, D., Gerish, S. and Sivan, A., (2005). Biodegradation of polyethylene by the thermophilic bacterium *Brevibacillus borstelensis*. *Jornal application microbiology*, **98**:1093-100.

Hay, N.J. (1995).The physical ageing of amorphous and crystalline polymers. *Journal of pure and applied chemistry*, **67**: 1855-1858.

Izer, A., Barany T., Varga, J. (2009). Developmentof woven fabricreinforced all PP composites with β-nucleated,homo and copolymer matrices. *Composites science and technology*, **69**: 2185-2192.

James, E.T. (1986). Atoms, radiation and radiation protection. Pergamon Press Inc: Newyork.

Kalfoglu, N.K. (1982). Thermal degradation and mechanical properties of PET blends. *Polymer science*, **20**: 1259.

Kathiresan, K. (2003). Polyethene and plastic degrading microbes from the mangrove soil. *Revision bio-tropical*, **51**(3): 629-634.

Khalid, M., Ratnam, C. T., Luqman, C. A., Salmiaton, A., Choolong, T. S. Y. and Jalaludin, H.(2009). Thermal and dynamic mechanical behavior of cellulose and oil palm empty fruit bunch (OPEFB)-filled polypropylene biocomposites; *Journal of polymer-plastics technology and engineering*, **48**: 1244-1251.

Kim, H.S., Yang, H.S., Kim, H.J. and Park, H.J. (2004). Thermo-gravimetric Analysis of Rice Husk Filled Thermoplastic Polymer Composites. *Journal of thermal analysis and calorimetry*, **76**: 395-404.

Kim, M., Pometto III, A.I. and Johnson, K.E. (1998). Degradation studies of novel degradable starch-polyethylene plastics containing oxidized polyethylene and pro-oxidant. *Journal of environmental polymers and degradation*, **2**: 27.

Konduri, M.K., Kurugarti, S.A., Jakkula, S.V., Rohiri, K.D. and Nasaru, M.L. (2004). Synergistic effect and photo-treatment on the rate of biodegradation of HDPE by indigeneous fungal isolates. *International Journal of biotechnology and biochemistry*, **6**: 157-174.

Labuzek, S., Nowak .B. and Pajak, J. (2003). The susceptibility of polyethylene modified with Bionelle to biodegradation by Filamentous Fungi. *Polymer journal of environmental studies*, **13**: 59-68.

Liu, N.C. and Baker, W.E. (1998). Water resistance, mechanical properties and biodegradability of methylated corn-starch. *Advanced polymer technology*, **11**: 249.

Lomakin, S.M., Rogovia, S.Z., Grachev, A.V., Prut, E.V. and Alexanyan, C.V. (2011). Thermal degradation of biodegradable blends of polyethylene with cellulose and ethycellulose. *Journal of Thermochimica Acta*, 1-8.

Mali, S., L. S. Sakanaka, F. Yamashita and Grossman. M. V. E. (2005). Water sorption and mechanical properties of cassava starch films and their relation to plastisizing effect. *Carbohydrate polymer*, **60**(3): 283-289.

Mancia, L. (1974). The Role of Additives in Plastics. Edwar Arnold, London.

Mani, R. and Bhattacharya, M. (1998). Properties of injected moulded starch/synthetic polymer blends-III. Effect of amylopectin to amylase ratio in starch. *European polymer journal*, **34**(10): 1467-1475.

Marias, C. and Villoutreix, G. (1998). Starch-polymer composites in degradable polymers. *Journal applications polymer science*, **69**: 1983.

Mears, P. (1954). Structure and bulk properties of polymers. *Journal of American chemistry society*, **76**: 3415.

Mehdi, B., Abdolreza, K., Shahrzad, K., Abdolrasoul, O. and Amir, H.J. (2010). Microbial degradable potato starch based LDPE. *African journal of biotechnology*, Vol. **9**(26): 4075-4080.

Ministry of environment, (2009). Plastic and waste oil production. Final report with the ministry of environment, Kenya.

Mohld, Z.A., Berry, J.P. (1994). Hygro-thermal aging studies of short carbon fibre reinforced nylon- 66. *Journal applications polymer science*, **51**: 2145-2155.

Morancho, J.M., Ramis, X., Fernandez, X., Cadenato, A. and Salla, J. M. (2006). Calorimetric and thermogravimetric studies of UV-irradiated polypropylene/starch-based materials aged in soil. *Polymer degradation and stability*, **6**: 9144-9151.

Norman, R.S., Fontera, S., Morris, P.J. (2002). Variability in *pseudomonas aeruginosa* lipo-polysaccharide expression during crude oil degradation. *Application environmental microbiology*, **68**(10): 5096-5103.

Osswald, T.A. and Menges, G. (2003). Material science of polymers for engineers, 2nd Edition. Hanser publishers, Munich.

Oyugi, B. (2007). Kenya says no to plastics. Ministry of environment, Kenya.

Painter, P.C. and Coleman, M.M. (1994). Fundamentals of polymer science. Technomic publishing company, Lancaster.

Plastic Europe, (2010). htt://www.plasticeurope.org/plastics-industry/market and economic.aspx.

Raghavan, D. (1995). Characterization of biodegradable plastics. *Polymer-plastic technology engineering*, **34**(1): 41-63.

Reyes-Romero, J., Albano, C., Davidson, E., Gonzalez, J., Ichazo, M. (2000). Proceedings of 8th polycharacterization. Texas, U.S.A.

Ribes-Greus, A. and Diaz-Calleja, R.J. (1987). Thermal characterization of photo-oxidised HDPE/Master-BI and LDPE/Master-BI blends buried in soil. *Journal applications polymer science*, **34**: 2819-2828.

Rodrig, H., Bush, A. and Lemon, M. (1975). Thermal analysis of high density polyethylene and low density polyethylene with enhanced biodegradability. *Journal polymer science*, **13**: 1921.

Rosato, T. (2001). The chemistry of side reactions and byproduct formation in the system NMMO/cellulose (Lyocell process). *Progress in polymer science*, **26**(9): 1763-1837.

Rutkowka, M., Heimowska, A., Krasowka, K., Jamik, H. (2002). Biodegradability of polyethylene starch blends in sea water. *Polymer journal environmental studies*, **11(**3): 267-274.

Sahebnaza, B.L., Swift, G. and Rutkowka, M. (2006). Biodegradation of thermally oxidized LDPE. *Polymer degradation and stability*, **81**: 231-262.

Sepe, P.M. (1992). Dynamic and mechanical analysis. *Journal of advanced materials and processes*, **12**: 32-34.

Shah, P.B., Bandopadhyay, S. and Bellare, J. R. (1995). Environmentally degradable starch filled LDPE. *Polymer degradation and stability*, **47**: 165-173.

Sielick, M., Focht, D., Martin J.P. (1978). Microbial degradation of [C 14 C] polystyrene and 1, 3-diphenyl butane. *Journal of microbiology*, **24**(7): 798-803.

Sperling, L.H. (1992). Introduction to physical polymer science, 2nd Editon. Academic press, Newyork: pp 320-323.

Stevens, P.M. (1990). An introduction in Polymer chemistry. John Wiley and sons, Newyork.

Strobl, G. (1997). The physics of polymers, concepts for understanding their structure and behavior, 2nd edition. Plenum press, Newyork: Chapter 5.

Tadros, R.M., Noureddini, H., Timm, D.C. (1999). Biodegradation of thermoplastic and thermaosetting polyesters from Z-protected glutanic acid. *Journal applications polymer science*, **74**(4): 3513-3521.

Tajividi, M. and Takemura, A. (2009). Effect of fibre content and type, compatibilizer, and heating rate on thermo-gravimetric properties of natural fibre HDPE composites, *Polymer composites*, **30**(9): 1226-1233.

Taylor, D.R. (2004). Mechanistic aspects of the effect of stress on the rate of photo-chemical degradation reactions in polymers. *Journal of macromology science part C polymer revision*, **44**(4): 351-88.

Tharanathan, R.N. (2003). Biodegradable films and composites coatings. *Trends in food science and technology*, **74**: 2701-2802.

Upreti, M.C. and Srivastava, R.B. (2003). A potential *Aspergillus* species for biodegradation of polymeric materials. *Curriculum science,* **84** (11): 1399-402.

Van, K.D. (1990). Properties of polymers, 3rd Edition. Elsevier publishing company, Newyork.

Villetti, M.K. and Parasama, P.H. (2002). Thermal properties of HDPE composites with natural fibres. *Polymer testing*, **21**: 181.

Vogel, G.,Fulcher, R.,Tumann, P. (1921). The temperature dependence law of viscosity in fluids. *Polymer structure and analysis*, **34**: 423.

Ward, I.M. and Hadley D.W. (1993.). An introduction to the mechanical properties of solid polymers. John Wiley and Sons Ltd, New York.

Williams, P.T. (1998). Waste treatment and disposal. *Polymer degradation and stability*, **24**: 431.

Wunderlich, B. and Seyler, R.J. (1994). Assignment of glass transition. American Society of Testing and Material (ASTM).

Yamada, O.K., Mukumoto, H., Katsuyama, Y., Saiganji, A. and Tani, Y. (2001). Degradation of polyethylene by a fungus; *Penicillium simplicissimum* Y K. *Polymer degradation and stability*, **72**: 323-327.

Zuchowska, D., Steller, R., Messner, W. (1999). Structure and properties of biodegradable polyolefin-starch blends. *Polymer degradation and stability*, **60**: 471-480.

APPENDICES

Appendix I: DMA and its features

Appendix II: Photograph of DMA 2980 model

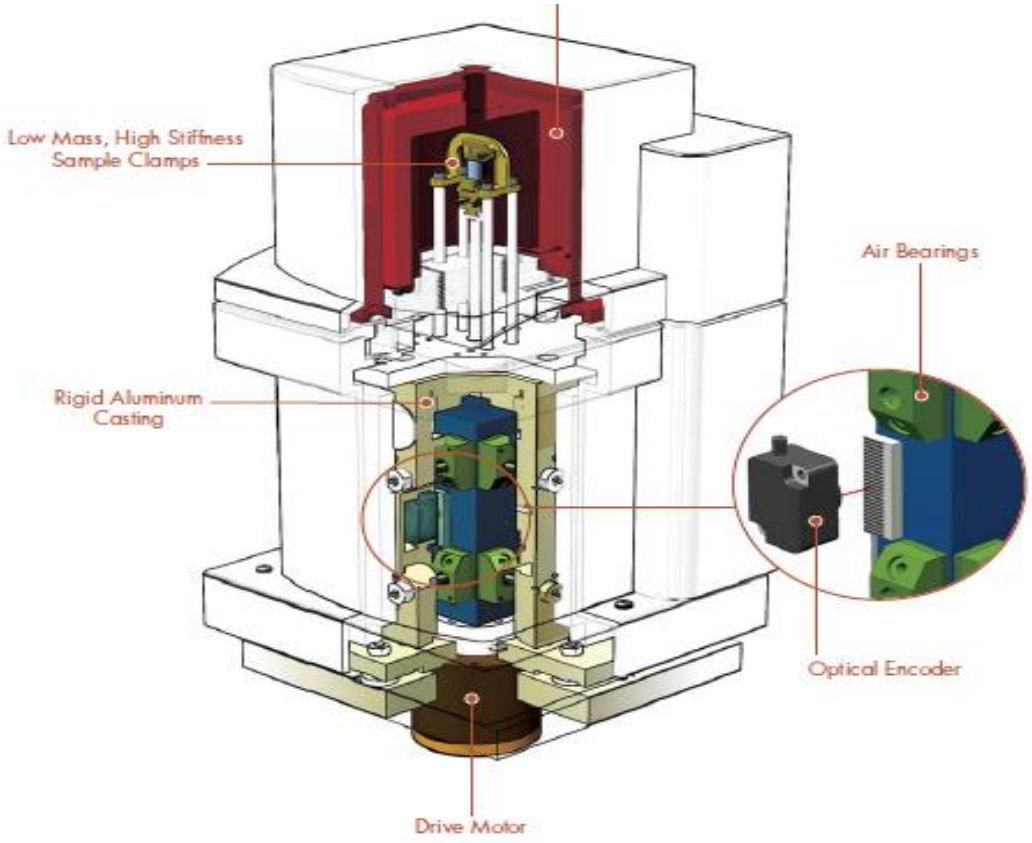

Appendix III: TGA measurement apparatus

Appendix IV: Photograph of inoculation process

On inoculation (0 days).

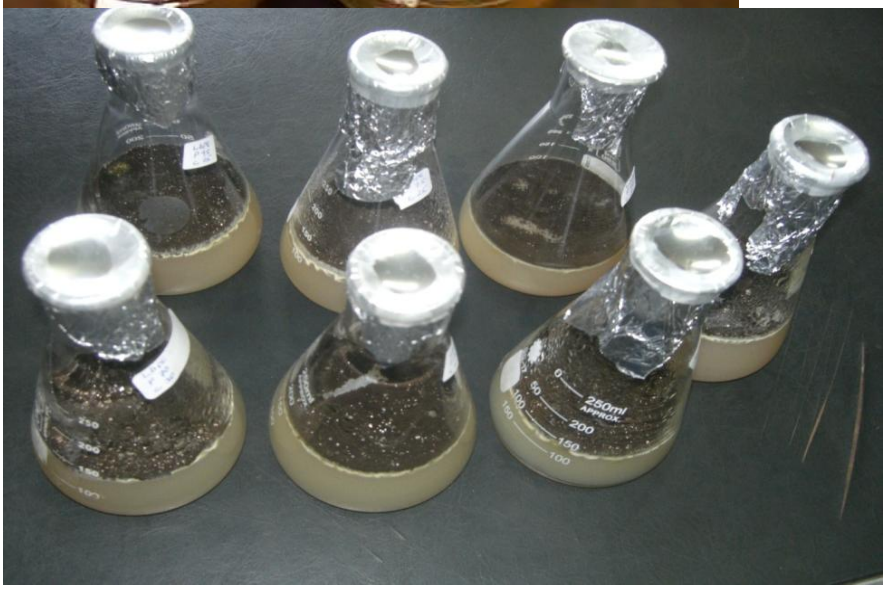

After 60 days.